Received: 30 July 2021 | Revised: 25 April 2022 | Accepted: 31 July 2022

DOI: 10.1111/fwb.13983

ORIGINAL ARTICLE

Freshwater Biology WILEY

Experimental thermocline deepening alters vertical distribution and community structure of phytoplankton in a 4-year whole-reservoir manipulation

Mary E. Lofton | Dexter W. Howard | Ryan P. McClure | Heather L. Wander | Whitney M. Woelmer | Alexandria G. Hounshell | Abigail S. L. Lewis | Cayelan C. Carey

Department of Biological Sciences, Virginia Tech, Blacksburg, Virginia, U.S.A.

Correspondence
Mary E. Lofton, Department of Biological Sciences, Virginia Tech, 926 W. Campus Dr., Blacksburg, VA 24060, U.S.A.
Email: melofton@vt.edu

Present address
Ryan P. McClure, School of the Environment, Washington State University, Pullman, Washington, U.S.A.

Alexandria G. Hounshell, National Centers for Coastal Ocean Science, National Ocean Service, National Oceanic and Atmospheric Administration, Silver Spring, Maryland, U.S.A.

Funding information
Global Change Center at Virginia Tech; National Science Foundation; Virginia Tech College of Science Roundtable Make-A-Difference Scholarship; Virginia Water Resources Research Center; Western Virginia Water Authority

Abstract

1. Freshwater phytoplankton communities are currently experiencing multiple global change stressors, including increasing frequency and intensity of storms. An important mechanism by which storms affect lake and reservoir phytoplankton is by altering the water column's thermal structure (e.g., changes to thermocline depth). However, little is known about the effects of intermittent thermocline deepening on phytoplankton community vertical distribution and composition or the consistency of phytoplankton responses to varying frequency of these disturbances over multiple years.
2. We conducted whole-ecosystem thermocline deepening manipulations in a small reservoir. We used an epilimnetic mixing system to experimentally deepen the thermocline via five short (24–72 hr) mixing events across two summers, inducing potential responses to storms. For comparison, we did not manipulate thermocline depth in two succeeding summers. We collected weekly depth profiles of water temperature, light, nutrients, and phytoplankton biomass as well as bottle samples to assess phytoplankton community composition. We then used time-series analysis and multivariate ordination to assess the effects of intermittent thermocline deepening due to both our experimental manipulations and naturally occurring storms on phytoplankton community structure.
3. We observed inter-annual and intra-annual variability in phytoplankton community response to thermocline deepening. We found that peak phytoplankton biomass was significantly deeper in years with a higher frequency of thermocline deepening events (i.e., years with both manipulations and natural storms) due to altered thermal stratification and more variable depth distributions of soluble reactive phosphorus. Furthermore, we found that the depth of peak phytoplankton biomass was linked to phytoplankton community composition, with certain taxa being associated with deep or shallow biomass peaks, often according to functional traits such as optimal growth temperature, mixotrophy,

and low-light tolerance. For example, *Cryptomonas* taxa, which are low-light tolerant and mixotrophic, were associated with deep peaks, while the cyanobacterial taxon *Dolichospermum* was associated with shallow peaks.

4. Our results demonstrate that abrupt thermocline deepening due to water column mixing affects both phytoplankton depth distribution and community structure via alteration of physical and chemical gradients. In addition, our work supports previous research that phytoplankton depth distributions are related to phytoplankton community composition at inter-annual and intra-annual timescales.
5. Variability in the inter-annual and intra-annual responses of phytoplankton to abrupt thermocline deepening indicates that antecedent conditions and the seasonal timing of surface water mixing may mediate these responses. Our findings emphasise that phytoplankton depth distributions are sensitive to global change stressors and effects on depth distributions should be taken into account when predicting phytoplankton responses to increased storms under global change.

KEYWORDS
epilimnetic mixing, functional traits, global change, storm, whole-ecosystem experiment

1 | INTRODUCTION

Phytoplankton in lakes and reservoirs are ecologically important organisms that are currently experiencing multiple global change stressors (Winder & Sommer, 2012). These stressors include nutrient (Smith, 2003) and sediment pollution (Donohue & Garcia Molinos, 2009), increased frequency and intensity of storms (Kirchmeier-Young & Zhang, 2020), and increased water temperatures (O'Reilly et al., 2015) that result in altered thermal stratification (Dokulil et al., 2021; Woolway & Merchant, 2019). Phytoplankton responses to these global change stressors range from changes in total biomass (Ho et al., 2019) to changes in phenology and seasonal succession (Henson et al., 2018) and changes in the presence and relative abundance (Carey et al., 2012; Winder & Sommer, 2012) or spatial distribution (Stockwell et al., 2020) of phytoplankton taxa. Because of the fundamental role phytoplankton play in freshwater ecosystem function, changes in the composition and distribution of phytoplankton communities can alter nutrient cycling (Cottingham et al., 2015), increase or decrease ecosystem productivity and dissolved oxygen levels (Diaz, 2001), and affect food quantity and quality for higher trophic levels (Danielsdottir et al., 2007). Global change stressors may also increase the prevalence of algal and cyanobacterial blooms (Ho & Michalak, 2020), which can have a variety of undesirable impacts including release of toxins (Chorus & Welker, 2021), unsightly surface scums, and taste and odour problems (Watson et al., 2016).

One important mechanism by which global change affects freshwater phytoplankton is via alteration of thermocline depth (Gray et al., 2019), which can occur either gradually due to changing air temperatures (Flaim et al., 2016; Kraemer et al., 2015) or abruptly due to storms (Jennings et al., 2012; Klug et al., 2012; Ren et al., 2020; Stockwell et al., 2020). Alteration of thermocline depth can affect the vertical distribution and composition of the phytoplankton community during the summer stratified period (Garneau et al., 2013; Jobin & Beisner, 2014), as phytoplankton biomass in many stratified lakes and reservoirs is shown to vary across depth, with peak biomass concentration often occurring well below the surface (Cullen, 2015; Hamilton et al., 2010; Latasa et al., 2017; Leach et al., 2018; Lofton et al., 2020). These biomass peaks form in response to vertical environmental gradients (e.g., of water temperature and light) within the water column (Cullen, 2015; Lofton et al., 2020; Longhi & Beisner, 2009; Reinl et al., 2020), and may be especially sensitive to global-change induced alteration of thermal stratification (Carey et al., 2012; Winder & Sommer, 2012).

Changes in thermocline depth may affect both the depth and spatial extent of phytoplankton biomass peaks (Figure 1; Beisner & Longhi, 2013; Jobin & Beisner, 2014; Leach et al., 2018; Lofton et al., 2020), as well as phytoplankton community composition (Jobin & Beisner, 2014; Lydersen & Andersen, 2007; Stockwell et al., 2020). Deepening thermoclines can increase the proportion of the water column where light availability and water temperature are suitable for phytoplankton growth (Huisman et al., 2004) or entrain nutrients from below the thermocline into the photic zone (Stockwell et al., 2020). As a result, thermocline deepening could either lead to: (1) a deeper phytoplankton biomass peak as phytoplankton shift to access entrained nutrients (Figure 1b; e.g., Garneau et al., 2013); or (2) a wider, more diffuse peak as some phytoplankton shift their depth to maximise entrained nutrient availability while others remain at shallow depths to maximise light availability (Figure 1c; e.g., Jobin & Beisner, 2014). Additionally, a thermocline that is shallower than the photic zone depth might favour taxa that are tolerant of high ultraviolet radiation and grow well at warm temperatures,

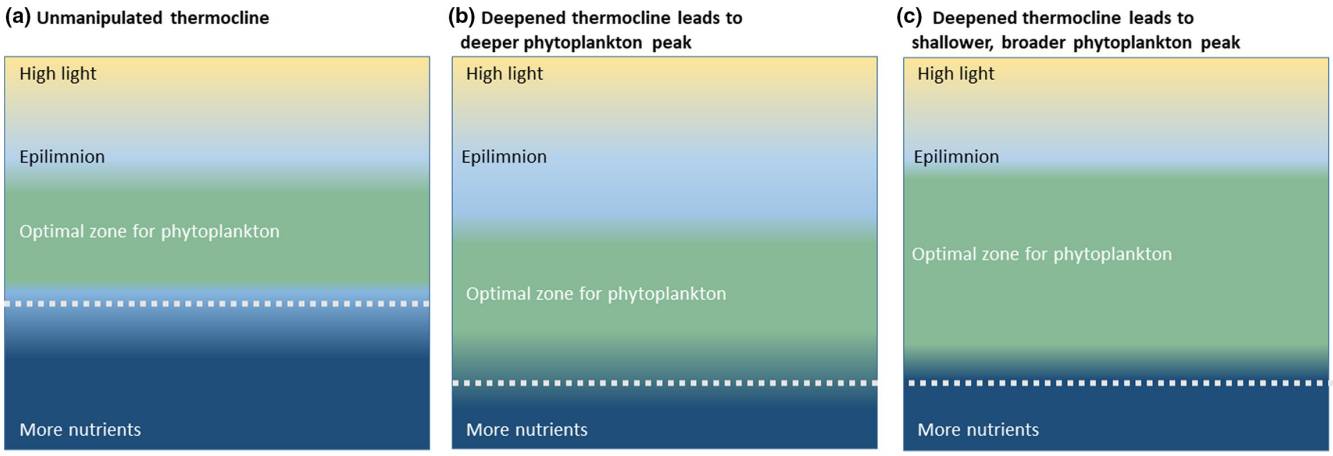

FIGURE 1 Conceptual figure illustrating hypothesised relationships between thermocline depth and peak phytoplankton biomass in the water column. (a) In an unmanipulated scenario, phytoplankton peak biomass occurs at a depth with optimal light, temperature, and nutrient conditions (optimal zone). In response to storm-induced thermocline deepening, (b) and (c) present two alternative hypotheses of phytoplankton responses. In (b), thermocline deepening shifts the location of the optimal zone for phytoplankton growth downwards as phytoplankton access nutrients that are entrained across the thermocline. In (c), thermocline deepening homogenises biomass across depth as some phytoplankton shift deeper to access entrained nutrients while others remain at shallow depths to maximise light availability, resulting in a broader optimal zone for phytoplankton. Gray dashed lines represent the thermocline. We note that storm events may lead to cooler water temperatures in the epilimnion (Stockwell et al., 2020), which is defined as the warmer surface waters of a thermally stratified water body.

while a deeper thermocline might favour taxa that are low-light tolerant and/or mixotrophic (Diehl et al., 2002; Huisman et al., 2004; Klausmeier & Litchman, 2001).

Gradual changes in thermocline depth due to air temperature warming and abrupt changes in thermocline depth due to storms probably evoke different phytoplankton responses at different time scales. Whole-ecosystem studies examining the response of phytoplankton to gradual thermocline deepening manipulations over multiple years, as might occur due to warming air temperatures, found that thermocline deepening affects the relative abundance of phytoplankton taxa and phytoplankton vertical distributions (Cantin et al., 2011; Jobin & Beisner, 2014; Lydersen & Andersen, 2007). Specifically, thermocline deepening increased species richness, decreased the abundance of chlorophytes and diatoms, and increased the abundance of mixotrophic dinoflagellates in an oligotrophic Norwegian lake over three years, although total phytoplankton biomass did not change (Lydersen & Andersen, 2007). Conversely, thermocline deepening led to increased chlorophyte abundance and total biomass (Cantin et al., 2011) and shallower, wider biomass peaks of phytoplankton (Jobin & Beisner, 2014) in different summers during a multi-year whole-ecosystem experiment in an oligotrophic lake in Québec, Canada. These contradictory findings highlight the possibility for multiple effects of thermocline deepening on phytoplankton community structure.

Variability in observed whole-ecosystem effects of a single abrupt thermocline deepening event on phytoplankton at daily to seasonal timescales (Garneau et al., 2013; Kasprzak et al., 2017; Planas & Paquet, 2016; Rinke et al., 2009; Wu et al., 2015) underscores the need for improved understanding of the potential cumulative effects of an increased frequency and intensity of multiple abrupt thermocline deepening events, especially at both intra-annual and inter-annual scales. Previous studies looking at single thermocline deepening events over periods of *c.* 24–48 hr due to high wind speeds, defined as winds with gusts reaching 5–12 m/s and sometimes co-occurring with precipitation, have observed conflicting results (Garneau et al., 2013; Kasprzak et al., 2017; Planas & Paquet, 2016; Rinke et al., 2009; Wu et al., 2015). Several studies that examined the effect of a single storm event on phytoplankton vertical distributions at the whole-ecosystem scale reported homogenisation of biomass across the epilimnion (warm surface waters) after a storm due to internal seiches, upwelling, and surface water mixing (Rinke et al., 2009; Wu et al., 2015; Planas & Paquet, 2016; Kasprzak et al., 2017; represented in Figure 1c). In contrast, another study did not report homogenisation, but instead a deepened biomass maximum after a storm (Garneau et al., 2013; represented in Figure 1b). Finally, abrupt experimental thermocline deepening caused increases in small, silica-containing flagellates and decreases in colonial, filamentous phytoplankton taxa, but inconsistent total biomass responses during a single summer (Lofton et al., 2019). These varying responses to single events highlight the pressing need to understand the *integrative* response of phytoplankton to an increased frequency and intensity of intermittent, abrupt thermocline deepening, such as might occur due to an increasing frequency of extreme storm events over multiple years due to global change.

The relationship between the frequency of abrupt thermocline disturbance and phytoplankton community structure over multiple summers has important implications for the predictability of phytoplankton community response to increased frequency and intensity of storms. Some research suggests that an increased frequency and intensity of thermocline deepening could result in greater rates of change in the presence and relative abundance of phytoplankton taxa (Pannard et al., 2008). Alternatively, as the frequency of thermocline deepening events increases, the phytoplankton community could shift to include more taxa that are well-adapted to mixed conditions

(Stockwell et al., 2020; Winder & Sommer, 2012). Furthermore, it is possible that both of these outcomes could be observed depending on the frequency of thermocline deepening events (Connell, 1978; Reynolds et al., 1993). A low frequency of thermocline deepening would lead to lower diversity via dominance of taxa well-adapted to stratified conditions, such as buoyant or motile taxa, while a high frequency of thermocline deepening would lead to lower diversity via dominance of taxa that are well-adapted to mixed conditions, such as silica-containing taxa, which sink out of stratified water columns (Klausmeier & Litchman, 2001). An important caveat to this framework is that the classification of thermocline deepening event frequency as *low*, *intermediate*, or *high* is subjective and depends on the life history traits of the phytoplankton taxa present (Fox, 2013; Reynolds et al., 1993). Additionally, it is likely that the antecedent conditions of thermocline deepening events, such as winter ice cover, the strength of thermal stratification, or cumulative year-to-date catchment precipitation, could affect phytoplankton community responses (Perga et al., 2018; Stockwell et al., 2020; Thayne et al., 2021). Examining the effects of thermocline deepening events at varying frequencies over multiple years will enhance our ability to predict phytoplankton community responses to future increases in extreme storm frequency.

We conducted multiple whole-ecosystem manipulations in which we experimentally deepened the thermocline of a small, eutrophic reservoir and examined the responses of phytoplankton depth distribution and community structure over 4 years. Our study addressed two research questions: (1) How do phytoplankton depth distribution and community structure change in response to an increased frequency of thermocline deepening events? and (2) What are the duration and consistency of these responses at intra-annual and inter-annual scales? We performed five thermocline deepening manipulations over two summers, and did not manipulate the thermocline in two additional reference summers. Throughout each summer, we monitored phytoplankton depth distribution and community structure at weekly intervals. We also measured a suite of physicochemical variables to assess responses to changes in gradients of light, temperature, and nutrients associated with thermocline deepening on weekly to inter-annual timescales.

2 | METHODS

2.1 | Study site

We conducted two summers of thermocline deepening manipulations (2016–2017), followed by two summers with no manipulations (2018–2019) in Falling Creek Reservoir (FCR), a small drinking water supply reservoir located in Vinton, VA, U.S.A. (37°18′12″ N, 79°50′14″ W; Figure 2). FCR is owned and operated by the Western Virginia Water Authority (WVWA). FCR has a maximum depth of 9.3 m (Figure 2), and is thermally stratified from approximately April to October each year with typical summer thermocline depths between 2–3 m when no thermocline deepening manipulations are conducted (Carey, Lewis, et al., 2021). Ice cover and inverse stratification occur intermittently during the winter months in most years (Carey, 2021). From May to September in 2016–2019, FCR's trophic state indicated mesotrophic to eutrophic conditions (following Carlson & Simpson, 1996): mean total phosphorus across the water column was 19 ±11 μg/L (1 *SD*), mean total nitrogen was 343 ±242 μg/L (Carey, Wander, et al., 2020), and mean Secchi depth was 2.0 ±0.7 m (Carey, Gerling, et al., 2020). Over the course of the study, water residence time in FCR had a median of 174 days (Carey, Breef-Pilz, et al., 2021; see Text S1), and the reservoir was managed to have a constant water level.

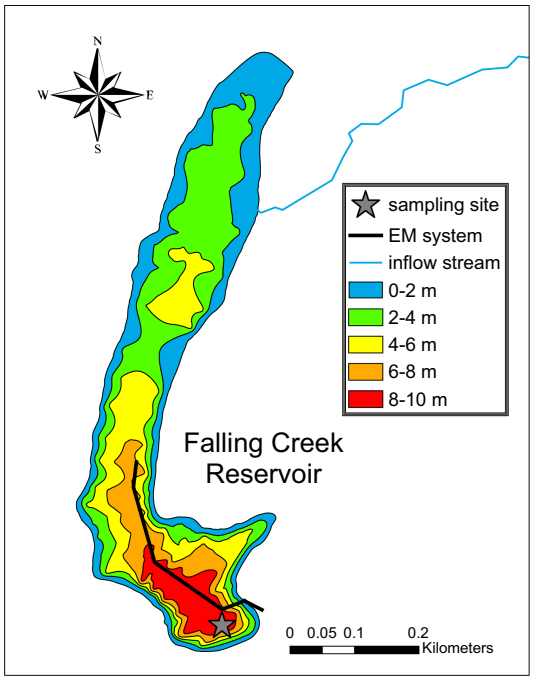

FIGURE 2 A map of Falling Creek Reservoir, located in Vinton, Virginia, U.S.A. The epilimnetic mixing (EM) system line shows the extent of the EM diffuser line within the reservoir that was used to implement the thermocline deepening manipulations.

2.2 | Thermocline deepening manipulations

An engineered bubble-plume epilimnetic mixing (EM) system was deployed in FCR for water quality management (see Visser et al., 2016 for a review on the use of artificial mixing for water quality management). The EM is installed at a depth of 5 m and extends throughout the lacustrine region of the reservoir (Figure 2). The system comprises an onshore air compressor coupled to a diffuser line of porous hose which can inject bubbles of atmospheric air at ambient air temperatures into the water column at rates up to 0.012 standard m^3/s (see Lofton et al., 2019 for an in-depth description of the EM system). Although slight lateral mixing and entrainment of water just below the EM is possible due to the configuration of the porous hose, the majority of the mixing effect from EM operation is limited to the top 5 m of the water column, preventing the reservoir from becoming destratified (Chen et al., 2018).

TABLE 1 Schedule of thermocline deepening manipulations, naturally occurring extreme storms, and field sampling from 2016–2019

	Thermocline deepening events								Sampling season	
Year	Date	Event type	Epilimnetic mixing	Intensity (SCMS)	Duration (hr)	Initial TD (m)	Final TD (m)	TD change (m)	Start date	End date
2016	5 May	Storm	–	–	–	3.1	4.2	1.1	2 May	20 Sept.
	29 May	EM	Continuous	0.012	6	3.3	3.8	0.5		
	27–28 June	EM	Continuous	0.007	24	3.4	5.3	1.9		
	25–27 July	EM	Continuous	0.004–0.012	56	2.7	5.5	2.7		
2017	30 May	EM	Continuous	0.007	24	3.9	5.1	1.2	15 May	4 Sept.
	10–12 July	EM	Intermittent (8 hr/day)	0.007	72	2.1	5.2	3.1		
2018	–		–	–	–	2.5	2.8	0.3	7 May	10 Sept.
2019	8 June	storm	–	–	–	3.1	4.2	1.1	6 May	11 Sept.

Abbreviations: EM, epilimnetic mixer; SCMS, standard m^3/s; TD, thermocline depth.

In 2016 and 2017, we conducted a total of five discrete, short (24–72-hr) manipulations in FCR to test operation of the EM in collaboration with the WVWA. Manipulations occurred in late May, late June, and late July of 2016 and in late May and early July of 2017 and had varied timing, intensity, and duration (Table 1) to provide the WVWA with information on the effects of EM operation under a range of conditions. These short, intense thermocline deepening manipulations are well-suited to simulate the abrupt changes in thermocline depth that can accompany storm events (e.g., Kasprzak et al., 2017) and contrast with previous empirical work examining phytoplankton response to thermocline deepening via gradual mixing (Cantin et al., 2011; Jobin & Beisner, 2014; Lydersen & Andersen, 2007). EM system testing was halted after 2 years and so the thermocline formed in the absence of manipulations during the summers of 2018 and 2019.

2.3 | Assessing effects of naturally occurring extreme storm events

To identify naturally occurring extreme storm events that might result in thermocline deepening, we measured wind speed (05103-L Wind Monitor, R.M. Young, Traverse City, MI, U.S.A.) and precipitation (TE525WS-L Rain Gauge, Texas Electronics, Dallas, TX, U.S.A.) at 1-min temporal resolution throughout the study period with a meteorological station (CR3000 Micrologger, Campbell Scientific, Logan, UT, U.S.A.) deployed on the dam of FCR (Figure 2; Carey, Breef-Pilz, et al., 2021).

To determine whether our thermocline deepening manipulations approximated naturally occurring storms, we calculated daily sums of precipitation and daily mean wind speed during the 4-year study period to identify *extreme* storm events. Extreme storms were defined as when both daily mean wind and summed precipitation were at or above the 95th percentile of all observation days (total $n = 572$) across the study period (following Doubek et al., 2021). Following this, we identified two extreme storm events during our 4-year study period: one on 5 May 2016 and one on 8 June 2019. We then examined thermocline depths immediately before and after these naturally occurring extreme storm events (within ±1 week) and compared them to changes in thermocline depth due to our manipulations.

Across the 4 years, manipulation summers experienced four (2016: three experimental, one natural) and two (2017: experimental) thermocline deepening events, whereas the reference summers experienced zero (2018) or one (2019: natural) thermocline deepening events, representing a substantial difference in thermocline deepening frequency between manipulation and reference summers (Table 1).

2.4 | Reservoir sampling

To assess the effect of thermocline deepening on phytoplankton, we collected weekly depth profiles of phytoplankton biomass and bottle

samples for microscope identification of phytoplankton taxa from May to September in 2016–2019. All sampling was conducted at the deepest site of the reservoir (Figure 2). Biomass depth profiles (*c*. 10 cm resolution) were collected using a FluoroProbe (bbe Moldaenke, Schwentinental, Germany; Catherine et al., 2012; Carey, Lofton, et al., 2021). FluoroProbes report total biomass as the summation of biomass across four spectral groups (green algae, brown algae, cyanobacteria, and cryptophytes; Beutler et al., 2002). For this study, we focused on total biomass profiles (vs. individual spectral groups) to represent the entire community's depth distribution patterns. Bottle samples for phytoplankton community composition were collected based on the depth of peak phytoplankton biomass according to FluoroProbe depth profiles using a 4-L van Dorn sampler (Wildco, Yulee, FL, U.S.A.). Samples were immediately preserved in opaque 250-ml high-density polyethylene (HDPE) bottles by adding *c*. 1% Lugol's iodine by volume for subsequent microscope analysis.

We also collected a suite of physicochemical variables each week to assess the effect of thermocline deepening over the 4-year study. We obtained *c*. 0.1 m-resolution depth profiles of water temperature (Carey et al., 2020, 2021 e) and photosynthetically active radiation (Carey, Gerling, et al., 2020; Carey, Lewis, et al., 2021) and measured Secchi depth (Carey, Gerling, et al., 2020). We also collected 1–2-m resolution depth profiles of water chemistry, including dissolved organic carbon (DOC), nitrate (NO_3), ammonium (NH_4), and soluble reactive phosphorus (SRP; Carey, Wander, et al., 2020). Detailed field sampling methods for physicochemical variables can be found in Text S2.

2.5 | Laboratory analyses

Phytoplankton bottle samples were counted on a Nikon Eclipse Ci microscope (Nikon, Minato City, Tokyo, Japan). Before counting, samples were permanently mounted on slides following Crumpton (1987). Samples were then counted at 400× until at least 300 natural units (either single cells or colonies) had been counted (Acker, 2002; Brierley et al., 2007). Phytoplankton were identified to genus and the first 10 natural units of each genus were measured and used to calculate biovolume following Hillebrand et al. (1999). All phytoplankton microscopy was conducted by M.E.L.

All soluble nutrient and dissolved organic carbon samples were analysed following standard methods within 6 months of collection (Carey, Wander, et al., 2020; Text S3). All data associated with this study are published in the Environmental Data Initiative repository (Carey, 2021; Carey et al., 2020b, 2021b, c, d, e; Lofton et al., 2021).

2.6 | Calculation of phytoplankton community and distribution metrics

We calculated multiple metrics to describe both phytoplankton biomass depth distributions and community composition at the depth of maximum biomass. First, we used the fluorescence-based depth profiles to calculate the depth of maximum phytoplankton biomass (peak depth), the magnitude of biomass at that depth (maximum biomass), and width of the biomass peak (peak width) across depth (following Leach et al., 2018; Lofton et al., 2020). Peak width was calculated by determining the closest depth above and below the depth of maximum biomass where phytoplankton biomass concentration was less than or equal to the median concentration across the water column. The difference between these two depths was assigned as the peak width (see Figure S1 for a visual explanation of peak width calculation).

Second, we used phytoplankton count data to assess community composition at the peak depth. We determined genus richness and calculated the relative abundance and Shannon diversity of phytoplankton groups (diatoms, chlorophytes, chrysophytes, cryptophytes, cyanobacteria, desmids, dinoflagellates, euglenoids, raphids) at the peak depth on each sampling day. To assess potential changes in both the relative abundance and the presence/absence of genera over time, we also calculated Bray–Curtis and Jaccard dissimilarity between samples each week within each year using the *vegdist* function of the *vegan* package (Oksanen et al., 2020).

2.7 | Calculation of physicochemical metrics

We analysed field data to calculate metrics describing the temperature, light, nutrient, and carbon conditions in the reservoir following previous studies (Cullen, 2015; Jobin & Beisner, 2014; Leach et al., 2018; Lofton et al., 2020). Thermocline depth, Schmidt stability, buoyancy frequency, lake number, and Wedderburn number were calculated for temperature profiles at *c*. 1 m resolution using the R package *rLakeAnalyzer* (Winslow et al., 2019). In addition, we determined the water temperature at the peak depth and the phytoplankton bottle sample on each sampling day. Photic zone depth was determined from PAR depth profiles as the depth where 1% of incident surface light was available, and the coefficient of light attenuation (K_d) was calculated as the slope of the best fit line of the natural logarithm of percent surface light plotted against depth (Wetzel & Likens, 1991). We also determined the percent of surface light that was available at the peak depth and phytoplankton bottle sample on each sampling day. To characterise carbon and nutrient conditions, we determined the concentration of DOC, dissolved inorganic nitrogen (calculated as the sum of NO_3 and NH_4), and SRP at the sampling depth closest to the peak depth and phytoplankton bottle sample on each sampling day, as well as the coefficient of variation of carbon and nutrients across the photic zone. We also determined the maximum carbon and nutrient concentrations across the photic zone on each sampling day, as well as the depth at which each concentration's maximum occurred.

2.8 | Assessing effects of increased thermocline deepening frequency

We used Anderson–Darling tests (Razali & Wah, 2011) to assess the effects of increased thermocline deepening frequency, including

both natural and experimental thermocline deepening events, on physicochemical and phytoplankton community structure metrics at the inter-annual scale. Anderson–Darling tests are used to assess significant differences between distributions of a variable without specifying the form of the distribution and give more weight to distribution tails or extreme values, permitting assessment of whether manipulations shifted both the mean and range of ecosystem variables (Razali & Wah, 2011). We considered a variable to be responsive to an increased frequency of thermocline deepening if variable distributions between summers with manipulations and reference summers were significantly different. All Anderson–Darling test *p* values were Holm–Bonferroni corrected for multiple comparisons (Holm, 1979).

2.9 | Analysis of phytoplankton depth distributions

We used autoregressive integrated moving average (ARIMA) models to assess how an increased frequency of thermocline deepening events affected phytoplankton depth distributions. ARIMA models are a well-established method for identifying the most important predictors of a response variable over time while accounting for autocorrelation (Hyndman & Athanasopoulos, 2018). We developed best-fit ARIMA models using physicochemical metrics to predict phytoplankton peak depth, peak width, and the magnitude of biomass at the peak depth over time. We fit models to the full time-series of depth distribution profiles (2016–2019) as well as to manipulation summers (2016–2017) and reference summers (2018–2019) separately to compare predictors of phytoplankton depth distributions between manipulation and reference summers and the full time-series. We did not fit ARIMA models to phytoplankton vertical distribution time series for each individual summer or before and after thermocline deepening events or extreme storms within a year because each summer's time series had fewer than 20 observations.

We developed a model selection algorithm based on the *auto.arima* function in the *forecast* package in R (Hyndman et al., 2021; Hyndman & Khandakar, 2008). Our algorithm compared models fit by *auto.arima* using all possible combinations of predictors to a global model using all predictors and a null model using no predictors. The algorithm then selected the model with the lowest corrected Akaike information criterion as well as all models within 2 units of the lowest corrected Akaike information criterion value (Burnham & Anderson, 2002). The models had a maximum of one autoregressive term (AR(1)), following results of partial autocorrelation functions (Hyndman & Athanasopoulos, 2018) calculated for each depth distribution metric (Figure S2).

We considered water temperature, light, and carbon and nutrient concentration metrics as potential predictors of phytoplankton peak depth, peak width, and the magnitude of biomass at the peak depth. We conducted pairwise Spearman correlations among all potential predictors; if two potential predictors had a pairwise Spearman's $\rho \geq 0.7$, we selected the predictor that was most strongly correlated with the corresponding response variable (Table S1). The distributions of all predictors and response variables were checked for skewness, log-transformed if appropriate, and standardised to Z-scores before fitting ARIMA models. If a predictor was included in the best-fit model for manipulation summers but not reference summers or vice-versa, we considered that as evidence that thermocline deepening manipulations had increased or decreased the importance of that predictor in driving phytoplankton depth distribution characteristics. If a predictor was included in the best-fit model for both manipulation and reference summers and the estimated coefficients on that predictor had overlapping confidence intervals, we considered the predictor to be equally important in both manipulation and reference summers. Because all possible predictors were standardised to Z-scores, we were able to compare the values of estimated model coefficients for different predictors, and considered predictors with estimated coefficients farthest from zero to be the strongest predictors of phytoplankton depth distribution metrics.

2.10 | Analysis of phytoplankton community data

To relate phytoplankton community structure to physicochemical and phytoplankton depth distribution metrics, we conducted non-metric multidimensional scaling analyses (NMDS). We used NMDS because this ordination technique does not assume a multivariate normal distribution of community data and does not constrain ordination results based on environmental gradients (McCune & Grace, 2002), which was appropriate given the non-normal distribution of our data and our goal of assessing community responses to thermocline deepening. We used the *metaMDS* function with Bray–Curtis dissimilarity in the *vegan* package to perform NMDS analyses across all summers (2016–2019) as well as for each summer individually. This function provides the benefit of including several random starts of the NMDS ordination process to ensure a stable result (Oksanen et al., 2020). We assessed the stress of each ordination result to determine the minimum number of axes needed to adequately explain variability in community composition data (McCune & Grace, 2002).

We used one-way analysis of similarities (ANOSIM) with Bray–Curtis dissimilarity to assess phytoplankton community differences among summers and months, between manipulation and reference summers, and before and after thermocline deepening events and extreme natural storm events within a summer. ANOSIM tests are a good complement to NMDS ordinations because both rely on ranked dissimilarities (McCune & Grace, 2002). ANOSIM tests report an *R* statistic, where values approaching 0 indicate similar groups, values approaching 1 indicate dissimilar groups, and values less than 0 indicate greater dissimilarity within a group than among groups (McCune & Grace, 2002). We considered month of year to be a proxy for change in the phytoplankton community due to seasonal succession, and so conducting ANOSIM tests on both month of year and the periods before and after thermocline deepening events within a summer allowed us to compare the relative importance of seasonal succession and thermocline deepening manipulations at the intra-annual scale. Although an intense storm occurred on 5 May

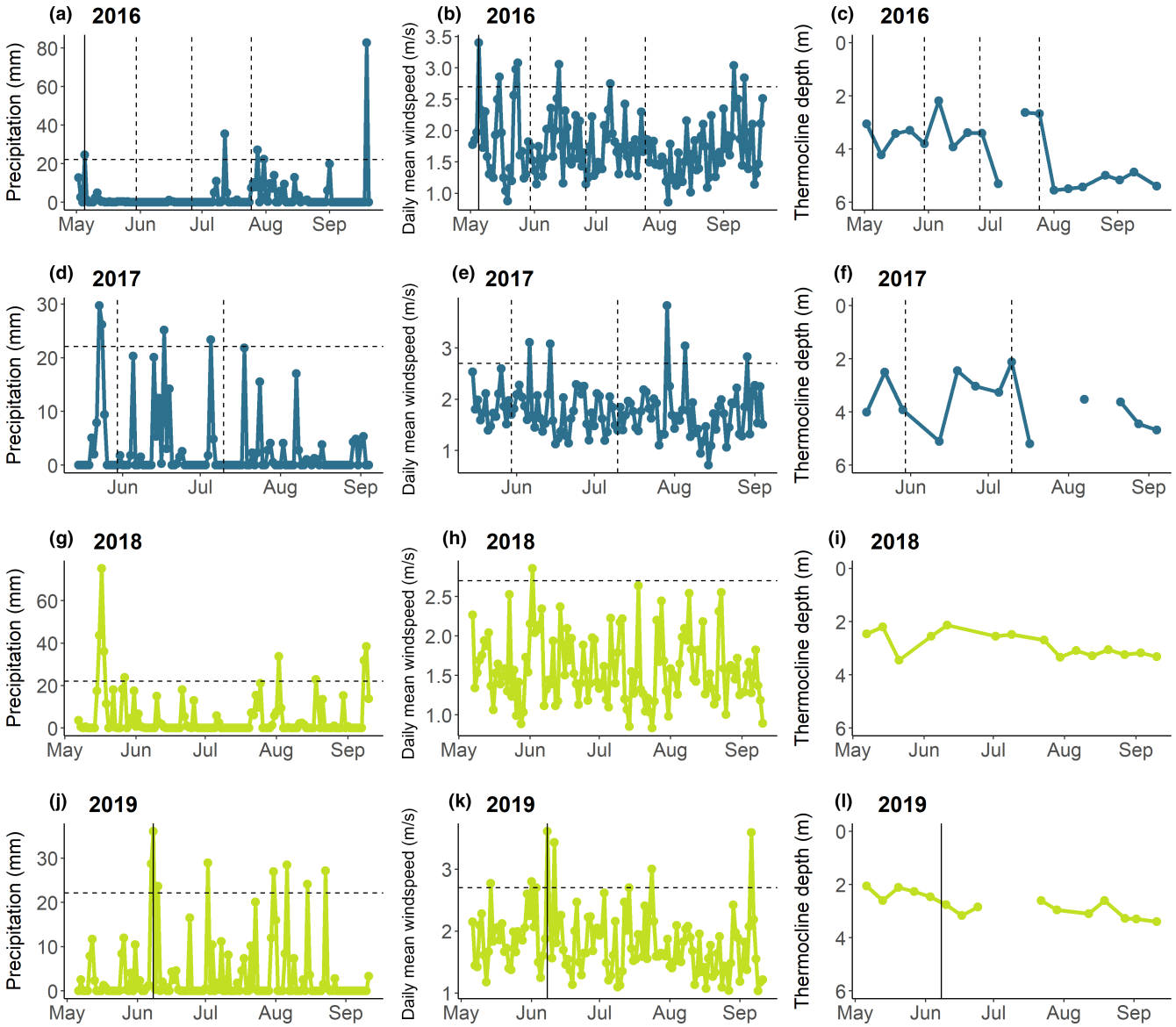

FIGURE 3 Daily summed precipitation (a, d, g, j), daily mean windspeed (b, e, h, k), and thermocline depth (c, f, i, l) for 2016 (a–c), 2017 (d–f), 2018 (g–i), and 2019 (j–l). Dashed horizontal lines represent the 95th percentile of daily precipitation (22.1 mm; a, d, g, j) and mean windspeed (2.7 m/s; b, e, h, k) observed during the 2016–2019 study period. Solid vertical lines represent naturally-occurring extreme storm events, defined as days with both daily precipitation and daily mean windspeed at or above the 95th percentile (5 May 2016 and 8 June 2019) and dashed vertical lines represent thermocline deepening manipulations (29 May 2016, 27–28 June 2016, 25–27 July 2016, 30 May 2017, 10–12 July 2017).

2016, no ANOSIM test was conducted for phytoplankton communities before and after this storm event due to insufficient pre-storm data ($n = 1$ pre-storm sampling point).

We also examined associations between phytoplankton genera and manipulation versus reference summers, periods before and after thermocline deepening events or intense storms within a summer, and each summer and month using indicator species analysis (*multipatt* function in the *indicspecies* package; De Cáceres et al., 2020). We selected the *multipatt* method for indicator species analysis because it permits species to be significantly associated with more than one group (e.g., a genus can be associated with both July and August communities; see De Cáceres et al., 2010).

Finally, we evaluated associations between physicochemical variables, depth distribution metrics, and phytoplankton community structure ordination output using the *envfit* and *ordisurf* functions in the *vegan* package. Briefly, the *envfit* function fits linear models between vectors of environmental variables and ordination scores and determines which fits are significant, and the *ordisurf* function fits a smoothed surface of an environmental variable to ordination scores using a generalised additive model (Oksanen et al., 2020).

All analyses were conducted in the R statistical environment (v. 4.0.3; R Core Team 2020). All analysis code is available on GitHub (https://github.com/melofton/FCR-phytos) and published via Zenodo (DOI: 10.5281/zenodo.6483433).

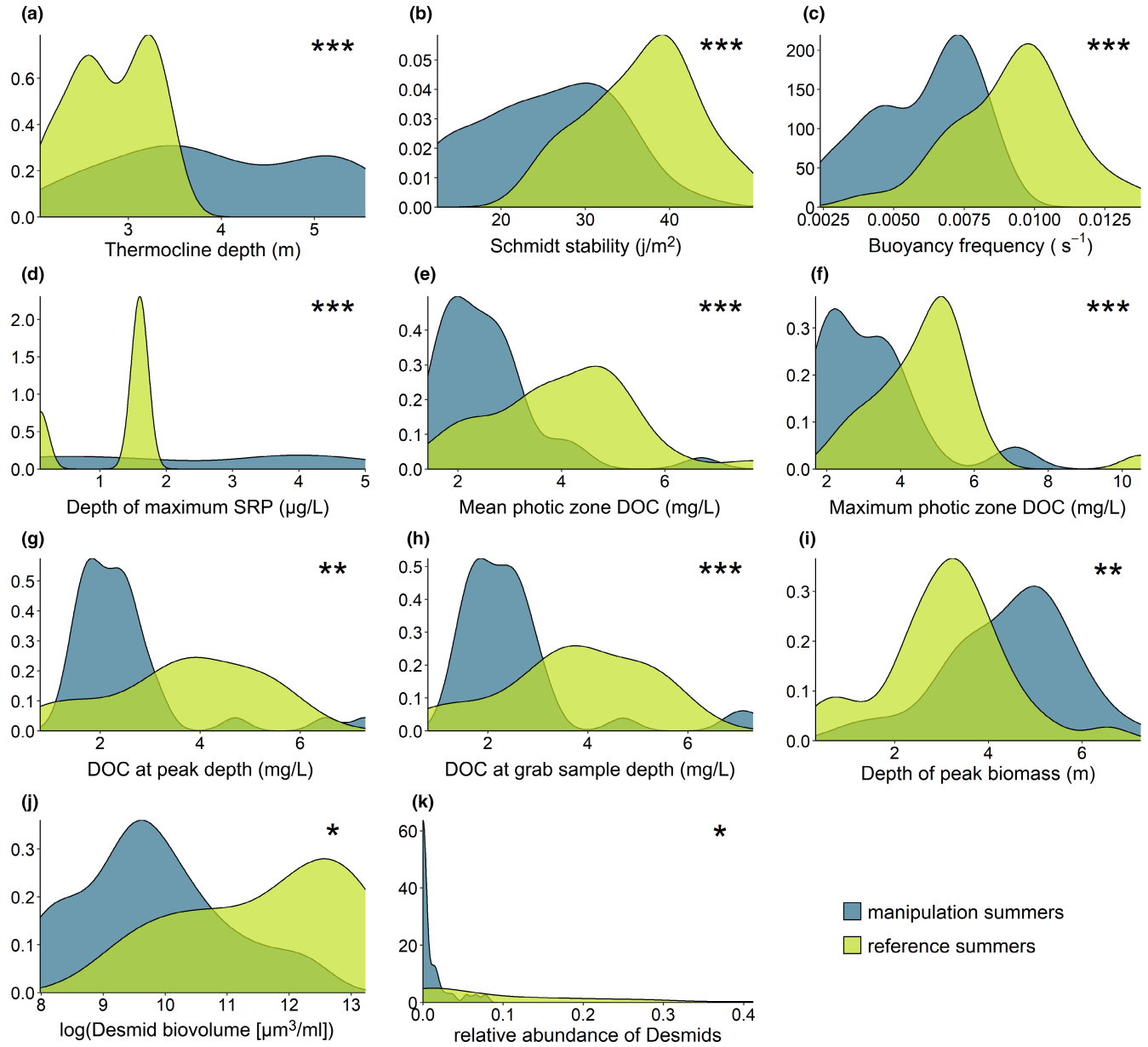

FIGURE 4 Distributions of physical (a–c), chemical (d–h), and biological variables (i–k) that had significantly different distributions in manipulation and reference summers according to Anderson–Darling tests, which assess significant differences between distributions of a variable without specifying the form of the distribution. Stars indicate significance levels between distributions of variables in manipulation and reference summers (*$p \leq 0.05$; **$p \leq 0.01$; ***$p \leq 0.001$). SRP, soluble reactive phosphorus; DOC, dissolved organic carbon

3 | RESULTS

3.1 | Thermocline deepening manipulations were representative of extreme storms

Comparison of our thermocline deepening manipulations with two naturally occurring extreme storms during the study period revealed that our manipulations reasonably approximated storm-induced thermocline deepening. A storm on 5 May 2016 deepened the thermocline by 1.1 m, and a storm on 8 June 2019 led to a 0.3 m deepening of the thermocline (Table 1; Figure 3), while changes in thermocline depth due to our manipulations ranged from 0.5 to 3.1 m (Table 1; Figure 3). Across all study summers, the thermocline depth ranged from 2.1 to 5.5 m and tended to be deepest in August and September due to seasonal cooling (Figure 3c,f,i,l).

3.2 | Increased frequency of thermocline deepening altered physicochemical variables

Multiple thermocline deepening manipulations in 2016 and 2017 significantly altered the summer thermal structure of FCR compared to reference summers, despite the occurrence of an extreme storm event in 2019 (Figures 4 and S3; Table S2). The distribution of observed thermocline depths was both deeper and more variable in manipulation summers (Figures 3c,f,i,l and 4a; adjusted

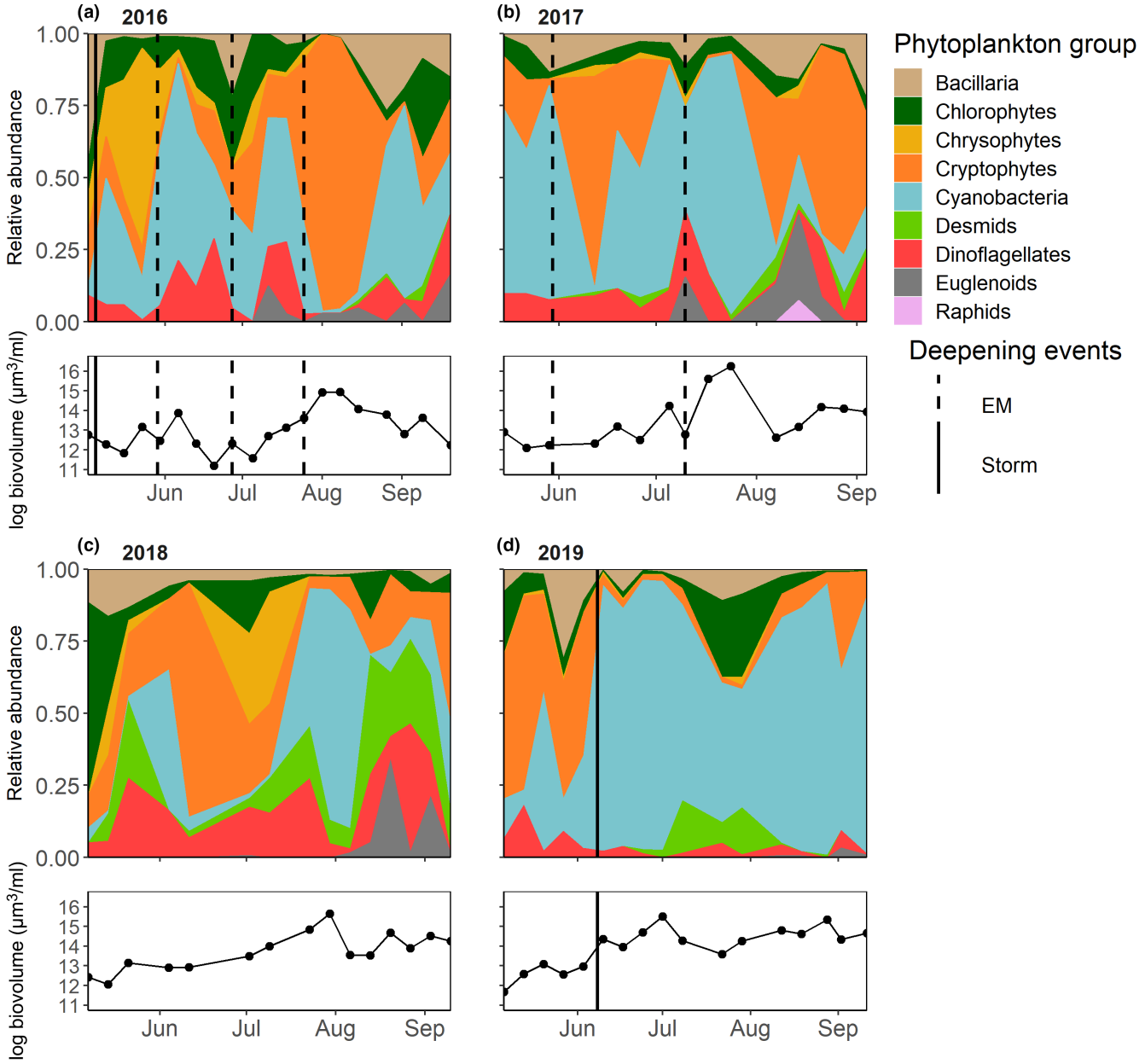

FIGURE 5 Time series of relative abundance of phytoplankton divisions and total biovolume for (a, b) manipulation summers and (c, d) reference summers. Thermocline deepening manipulations in 2016 and 2017 are denoted with dashed black vertical lines, and naturally occurring extreme storms in 2016 and 2019 are denoted with solid black vertical lines.

Anderson–Darling $p = 3.4 \times 10^{-4}$). We note that while the EM system was deployed at 5 m, operation of the system led to a limited degree of lateral mixing and entrainment of water from below the EM system in addition to mixing of water above the system deployment depth (Chen et al., 2018), leading to post-manipulation thermocline depths of up to 5.5 m (Table 1).

An increased frequency of thermocline deepening decreased the distributions of Schmidt stability and buoyancy frequency towards less strongly stratified conditions (Figure 4b,c; Table S2; Schmidt stability adjusted Anderson–Darling $p = 2.6 \times 10^{-5}$; buoyancy frequency adjusted Anderson–Darling $p = 3.4 \times 10^{-6}$). There were no significant changes in the distributions of lake number or Wedderburn number between manipulation and reference summers (Table S2).

Soluble reactive phosphorus depth distributions across the photic zone were different in manipulation and reference summers (Table S2; Figure 4d). The distribution of depths where maximum SRP was observed in the photic zone shifted deeper and was more variable in manipulation summers (Figure 4d; adjusted Anderson–Darling $p = 7.3 \times 10^{-4}$). The magnitude of maximum summer SRP concentration in the photic zone ranged from 7 to 20 µg/L across all summers, and the distribution of these concentrations was not different between manipulation and reference summers (Table S2).

Several metrics of DOC in the photic zone exhibited different distributions between manipulation and reference summers (Figure 4e–h; Table S2). The distributions of observed mean photic zone DOC as well as DOC at the peak depth and phytoplankton bottle samples were

TABLE 2 Best-fit autoregressive integrated moving average (ARIMA) models predicting depth of peak phytoplankton biomass, peak width, and the magnitude of maximum biomass across all summers (*all*; 2016–2019), as well as manipulation (abbreviated as *man*; 2016–2017) and reference (*ref*; 2018–2019) summers. ARIMA models that were within 2 corrected Akaike information criterion (AICc) units of the best-fit models for each response variable and time period are reported in Table S3. Note that AICc values in this table cannot be compared as models were fit to different datasets. However, RMSE values for model fits for each depth distribution metric are comparable. SRP, soluble reactive phosphorus; K_d, light attenuation coefficient; DIN, dissolved inorganic nitrogen; DOC, dissolved organic carbon; CV, coefficient of variation; AR(1), an autoregressive term with a time lag of one; MA(1), a first-order moving average term. Model order is specified as (*p*,*d*,*q*) where *p* is the order of the autoregressive term, *d* is the order of the integration term, and *q* is the order of the moving average term

		ARIMA model structure			Coefficient values of predictor variables									
					Thermal environment				Light environment	Chemical environment				
Metric	**Years**	**Order**	**Terms**										**AICc**	**RMSE**
			AR(1)	*MA(1)*	*Thermocline depth (m)*	*Schmidt stability ($J\ m^{-2}$)*	*Lake number*	*Wedderburn number*	*K_d (m^{-1})*	*Depth of max. SRP in photic zone (m)*	*Depth of max. DIN in photic zone (m)*	*Depth of max. DOC in photic zone (m)*		
Peak depth (m)	All	(1,1,1)	0.47 ± 0.18	−0.94 ± 0.05	−0.27 ± 0.12	–	−0.57 ± 0.13	0.25 ± 0.10	0.19 ± 0.13	0.03 ± 0.11	−0.02 ± 0.13	0.06 ± 0.10	121.54	0.65
	Man	(0,0,0)	–	–	–	–	−0.53 ± 0.17	–	–	0.27 ± 0.17	−0.02 ± 0.18	−0.22 ± 0.17	64.08	0.75
	Ref	(0,0,0)	–	–	–	–	−0.32 ± 0.19	–	−0.42 ± 0.20	0.06 ± 0.19	–	0.17 ± 0.17	68.61	0.79
						Buoyancy frequency (s^{-1})	*Lake number*	*Wedderburn number*	*K_d (m^{-1})*	*CV of SRP in photic zone*	*CV of DIN in photic zone*	*CV of DOC in photic zone*		
Peak width (m)	All	(0,0,0)	–	–	–	−0.31 ± 0.11	–	–	−0.13 ± 0.12	–	–	−0.11 ± 0.11	191.64	0.93
	Man	(0,0,0)	–	–	–	−0.26 ± 0.15	–	–	–	0.18 ± 0.15	–	–	102.35	0.91
	Ref	(0,0,0)	–	–	–	−0.22 ± 0.17	–	–	−0.34 ± 0.18	–	–	−0.16 ± 0.18	95.16	0.93
			AR(1)	*MA(1)*	*Water temperature at the depth of peak biomass (°C)*	*Buoyancy frequency (s^{-1})*	*Lake number*	*Wedderburn number*	*% of surface light at depth of peak biomass*	*SRP concentration at depth of peak biomass (μg/L)*	*DIN concentration at depth of peak biomass (μg/L)*	*DOC concentration at depth of peak biomass (mg/L)*		
Max. biomass (μg/L)	All	(1,0,0)	0.53 ± 0.11	–	0.61 ± 0.16	–	0.17 ± 0.11	–	−0.43 ± 0.14	−0.05 ± 0.11	–	–	145.17	0.69
	Man	(1,0,1)	0.57 ± 0.16	0.62 ± 0.30	–	–	0.20 ± 0.10	−0.22 ± 0.06	–	–	0.10 ± 0.07	–	79.23	0.54
	Ref	(0,0,0)	–	–	1.1 ± 0.17	–	–	–	−0.75 ± 0.15	−0.24 ± 0.15	–	–	64.09	0.67

narrower and shifted towards lower DOC concentrations, so that rather than having a majority of observation fall close to 4 mg/L as in reference summers, the majority of observations fell close to 2 mg/L in manipulation summers (Figure 4e,g,h). The distribution of observed maximum photic zone DOC also shifted towards lower concentrations in manipulation years, although some higher concentrations (*c.* 6–8 mg/L) were observed in manipulation years (Figure 4f). No other metrics of water temperature, light, nutrients, or carbon were significantly different between manipulation and reference summers (Table S2).

3.3 | Deeper maximum phytoplankton biomass in manipulation years

Phytoplankton depth distributions were altered by an increased frequency of thermocline deepening (Figure 4i; Table S2) in support of the hypothesis presented in Figure 1b. Peak depth ranged from 0.31–7.25 m in 2016–2019, and the distribution of observed peak depths was deeper in manipulation summers than in reference summers (Figure 4i; adjusted Anderson–Darling $p = 2.4 \times 10^{-3}$).

Increased thermocline deepening frequency did not affect distributions of observed peak width or maximum biomass (Table S2). High-biomass events (i.e., blooms, defined as >2*SD* greater than the mean biomass for 2016–2019) occurred in 2017 and 2019 (Figures 5 and S4), indicating that manipulations neither consistently caused nor prevented bloom formation. However, the distributions of observed desmid biovolume and relative abundance differed between manipulation and reference summers, with the distributions of biovolume and relative abundance of desmids shifted upwards in reference summers (Figure 4j,k; desmid biovolume adjusted Anderson–Darling $p = 0.02$; desmid relative abundance adjusted Anderson–Darling $p = 0.02$).

3.4 | Predictors of depth distributions differed between manipulation and reference summers

Physicochemical predictors of phytoplankton depth distributions differed between manipulation and reference summers (Tables 2 and S3). Overall, metrics of thermal stratification and nutrient conditions were important in best-fit ARIMA models for all summers, while metrics characterising the light environment tended to be more important in models fit for reference summers.

Lake number was the strongest predictor of peak depth in manipulation summers, while the rate of light attenuation (K_d) was a better predictor in reference summers (Table 2). In manipulation summers, peak depth decreased as lake number increased, consistent with our finding from Anderson–Darling tests that the distribution of observed peak depths shifted deeper during manipulation summers characterised by less strongly stratified conditions. The depth of peak biomass in manipulation summers was positively associated with the depth of maximum SRP in the photic zone and negatively associated with the depth of maximum DOC in the photic zone. During reference summers, biomass peaks were shallower when the light attenuation rate was high and the water column was highly stratified (Table 2). Finally, biomass peaks in reference summers were also positively related to the depth of maximum DOC in the photic zone (Table 2). Important predictors of peak depth for all summers included multiple metrics of thermal structure (thermocline depth, lake number, and Wedderburn number) and K_d.

The predictors of peak width and maximum biomass differed between manipulation and reference summers (Table 2). During manipulation years, peaks were narrowest when buoyancy frequency was high. In reference summers, peaks were narrowest when light attenuation rates were high. During manipulation summers, the strongest predictor of maximum biomass at the depth of peak biomass were the AR(1) and MA(1) terms, indicating autocorrelation of both maximum biomass observations and predictive errors at the previous timestep. In reference summers, maximum biomass was highest when water temperatures were high.

3.5 | Increased thermocline deepening affects inter-annual phytoplankton community composition

Thermocline deepening manipulations were associated with inter-annual changes in phytoplankton community composition, according to NMDS ordination results (Figure 6). We found that phytoplankton community composition at the inter-annual scale was sufficiently explained by three NMDS ordination axes (stress = 0.11). Although there was some overlap among communities each year, phytoplankton communities in manipulation years clustered towards the top and right of ordination space in the first and second dimensions of the 2016–2019 NMDS ordination (Figure 6a). Phytoplankton communities in manipulation years were associated with the occurrence of experimental

FIGURE 6 (a) First and second and (b) second and third axes of non-parametric multidimensional scaling (NMDS) ordination for phytoplankton communities across all summers (2016–2019), as well as NMDS ordination results for individual summers: (c) 2016, (d) 2017, (e) 2018, and (f) 2019. Grey and black arrows in (a) and (b) are fitted vectors of physicochemical variables plotted at a $p < 0.01$ significance level, with variables that differed in manipulation versus reference summers in black. Arrow length indicates the relative correlation strength of each physicochemical variable with phytoplankton community structure. D1 indicates the inter-annual manipulation regime, coded as 0 for reference summers and 1 for manipulation summers. D2 indicates the intra-annual manipulation regime, coded as 0 for reference years or pre-thermocline deepening during manipulation summers, 1 for after the first thermocline deepening event within a manipulation summer, 2 after the second thermocline deepening event, and 3 after the third thermocline deepening event. Other vector label abbreviations: Biom, magnitude of biomass in the phytoplankton biomass peak; LN, lake number; WN, Wedderburn number; Mo, month; N2, buoyancy frequency; PD, phytoplankton biomass peak depth; T, water temperature at the depth of the phytoplankton bottle sample (peak biomass depth); Yr, year. The month colour legend in (e) applies to all sub-plots. EM, epilimnetic mixing

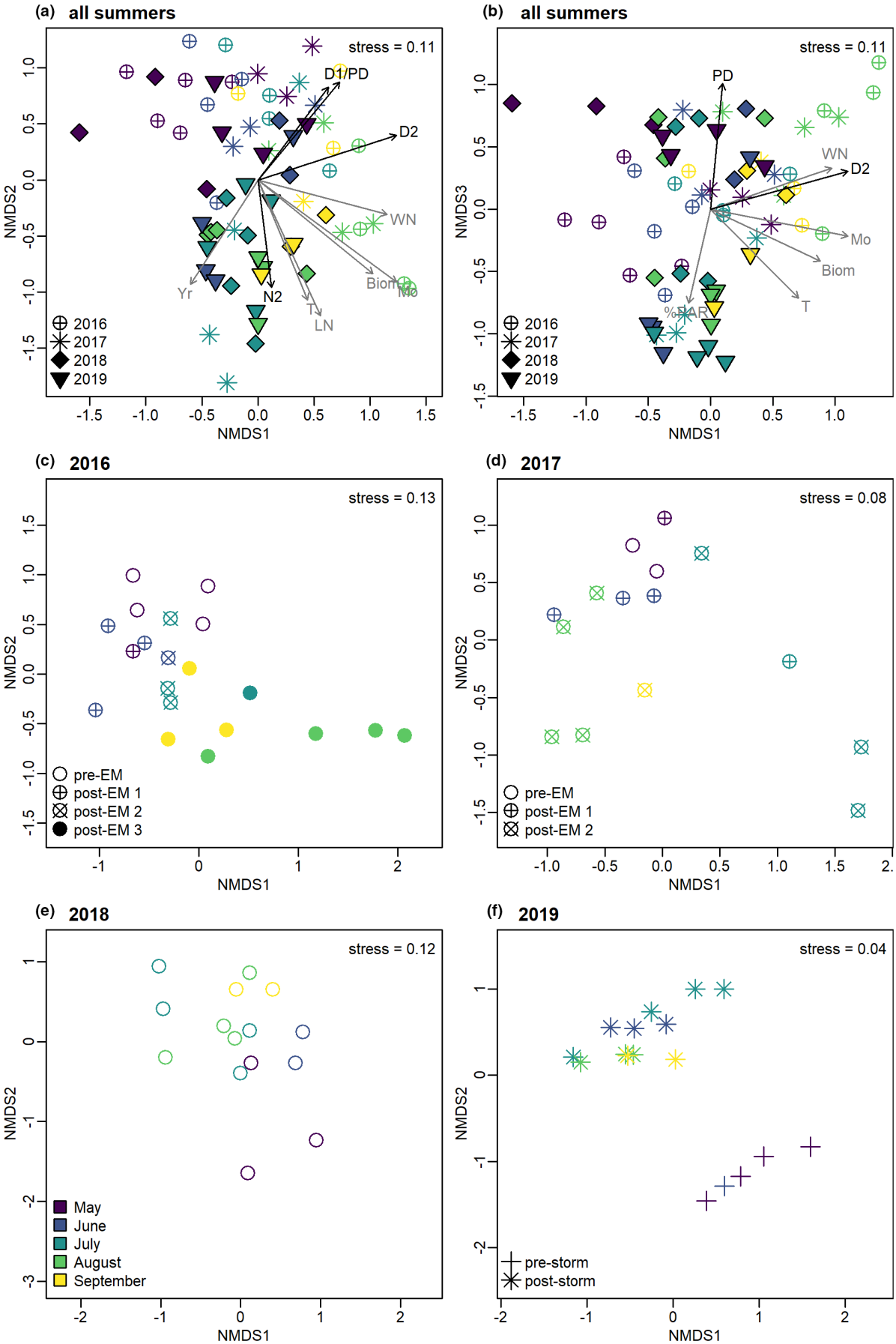

thermocline deepening events (Figure 6a). In the first and third dimensions, phytoplankton communities in manipulation years clustered to the centre-left (2016) and top-right (2017; Figure 6b). Experimental thermocline deepening within a summer, peak depth, and month of year were associated with phytoplankton community structure in the first and third dimensions of the NMDS output (Figure 6b).

We found that phytoplankton community composition at the intra-annual scale was sufficiently explained by two NMDS ordination axes for each year (2016 stress = 0.13; 2017 stress = 0.08; 2018 stress = 0.12; 2019 stress = 0.04). Water temperature was the physicochemical variable most often strongly associated with phytoplankton community composition in NMDS ordination results for individual summers (Figures 6 and 7; Table S4).

3.6 | Increased thermocline deepening affects intra-annual phytoplankton community composition

Within each summer, phytoplankton communities changed from month to month (Figure 6; Table 3), as expected due to seasonal succession. Overall, summer months within manipulation years were more dissimilar (2016 R = 0.50 and 2017 R = 0.47) than summer months within reference years (2018 R = 0.24 and 2019 R = 0.33). In 2016, phytoplankton communities after the second and third deepening events in late June and July were different from pre-deepening (May-early June) phytoplankton communities (ANOSIM R = 0.57 and 0.58, respectively; Figure 6c; Text S4; Table S6). Additionally, phytoplankton communities before and after the naturally occurring extreme storm event in 2019 were substantially different (R = 0.98; Figure 6f). Pairwise ANOSIM results for year, months within a year, thermocline deepening periods within a year, and month of year across years are presented in Tables S5, S6, S8, and S9, respectively.

3.7 | Phytoplankton taxa associated with reference summer phytoplankton communities

Although the distributions of observed total genera richness in phytoplankton samples were not different between manipulation and reference summers (adjusted Anderson–Darling p = 1; Table S2), indicator species analysis revealed that seven genera were associated with reference summer conditions, three of which were desmids (*Staurastrum* and *Staurodesmus* in 2018 and *Spondylosium* in 2019). Other taxa associated with phytoplankton communities in reference summers included cryptophyte taxa (*Rhodomonas*) and green algae taxa (*Oocystis*, *Monomastix*, *Selenastrum*). No taxa were significantly associated with manipulation summer communities. From 2016–2019, genus richness in phytoplankton samples from the depth of maximum biomass ranged from 7 to 18 genera, and a total of 65 genera were observed from 2016–2019 (Table S7; see Text S5 for further description of phytoplankton community structure).

Indicator analysis revealed that several taxa were associated with post-storm and post-thermocline-deepening communities. A colonial, filamentous cyanobacterium (*Dolichospermum*), a single-celled, flagellated mixotroph (*Rhodomonas*), and a centric diatom (*Cyclotella*) were associated with post-storm communities in 2019, as well as following thermocline-deepening manipulations in 2016. Congruence between taxa associated with late summer communities and post-storm or post-thermocline-deepening communities (e.g., *Dolichospermum*, *Trachelomonas*, *Cyclotella*; Text S4) emphasises the difficulty of disentangling the effects of thermocline deepening or extreme storms from seasonal succession (Text S4; Tables S6, S8, S9).

3.8 | Phytoplankton community structure differed between deep and shallow biomass peaks

Different peak depths were associated with different phytoplankton communities (Table 3; Figure 7). Aggregated across 2016–2019, median peak depth was 3.6 m, and the inter-quartile range of peak depths was 3.1–4.9 m. The top two dominant genera across the 2016–2019 sampling period (*Cryptomonas* and *Dolichospermum*) were associated with deep and shallow peaks, respectively, according to indicator species analysis (Figure 7a,b). In addition to *Cryptomonas*, one green algae genus (*Elakatothrix*) was associated with peaks deeper than 3.6 m, while a diverse suite of genera other than *Dolichospermum*, including green algae (nanoplankton <5 μm GALD, *Selenastrum*), dinoflagellate (*Parvodinium*), diatom (*Nitzchia*), and cryptophyte (*Rhodomonas*) taxa were associated with peaks shallower than 3.6 m.

FIGURE 7 Non-parametric multidimensional scaling (NMDS) ordinations overlain with the smooth surface plane for biomass peak depth for all summers (a and b), 2016 (c), 2017 (d), 2018 (e), and 2019 (f). Plane contours are shown for median peak depth from 2016 to 2019 (3.6 m, plotted in grey) as well as the inter-quartile range of peak depth (first quartile = 3.1 m, plotted in light grey; third quartile = 4.9 m, plotted in dark grey). Genera shown in text were associated with either shallow (<3.6 m) or deep (>3.6 m) peak depth in indicator species analysis. Genus abbreviations: Aph, *Aphanocapsa*; Ast, *Asterionella*; Chl, small green algae nanoplankton (<5 μm greatest axial linear dimension); Cry, *Cryptomonas*; Cyc, *Cyclotella*; Dic, *Dictyosphaerium*; Dol, *Dolichospermum*; Ela, *Elaktothrix*; Eug, *Euglena*; Nit, *Nitzchia*; Par, *Parvodinium*; Rho, *Rhodomonas*; Sel, *Selenastrum*; Spo, *Spondylosium*. Black arrows in (c–f) show fitted vectors of physicochemical variables (significance level for vector plotting is p <0.01; arrow length indicates the relative correlation strength of each physicochemical variable with phytoplankton community structure). Arrows that overlap (c) are labelled with a single label for legibility. D2 indicates the intra-annual mixing regime, coded as 0 for reference years or pre-thermocline deepening during manipulation summers, 1 for after the first thermocline deepening event within a manipulation summer, 2 after the second thermocline deepening event, and 3 after the third thermocline deepening event. Other vector label abbreviations: Biom, magnitude of biomass in the phytoplankton biomass peak; DOC, concentration of dissolved organic carbon at the depth of peak biomass; Mo, month; N2, buoyancy frequency; PD, depth of peak biomass; SRP, concentration of soluble reactive phosphorus at the depth of peak biomass; T, water temperature at the depth of peak biomass.

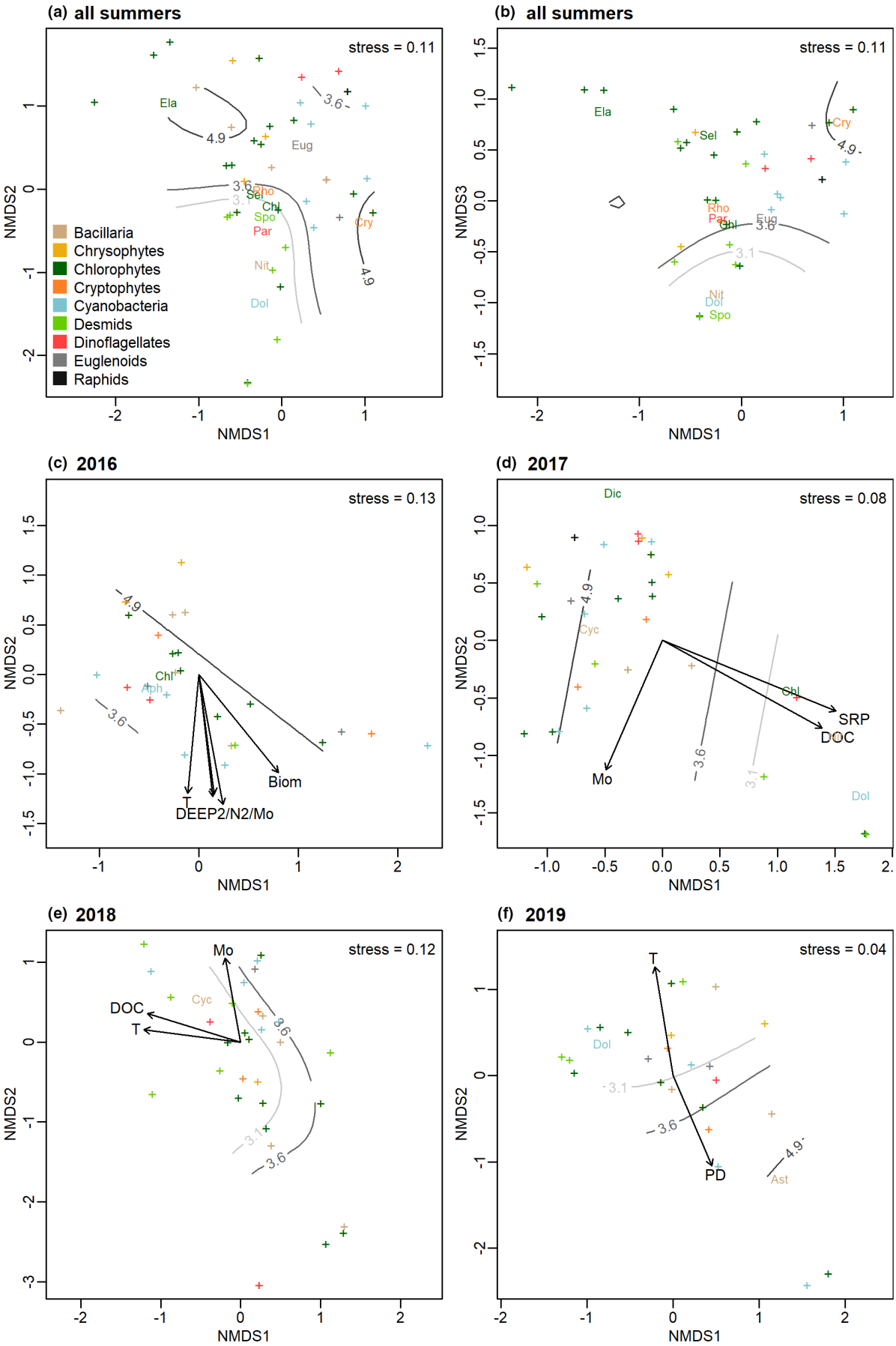

TABLE 3 One-way analysis of similarities (ANOSIM) results conducted on Bray–Curtis dissimilarity based on phytoplankton community data were assessed for differences based on grouping by year, month, two thermocline deepening indicator variables, and one peak depth indicator variable

	Year		Month		DEEP1[a]		DEEP2[b]		Peak biomass depth[c]		Pre- and post-intense storms[d]	
NMDS input data	*R*	*p*	*R*	*p*	*R*	*p*	*R*	*p*	*R*	*p*	*R*	*p*
2016–2019	**0.20**	1×10^{-4}	**0.19**	1×10^{-4}	**0.15**	2×10^{-4}	0.06	0.19	**0.28**	1×10^{-4}	–	–
2016	–	–	**0.50**	1×10^{-4}	–	–	**0.30**	9×10^{-3}	0.03	0.32	–	–
2017	–	–	**0.47**	1×10^{-3}	–	–	−0.05	0.58	**0.46**	**0.01**	–	–
2018	–	–	**0.24**	**0.04**	–	–	–	–	−0.02	0.47	–	–
2019	–	–	**0.33**	**0.01**	–	–	–	–	**0.78**	6×10^{-4}	**0.98**	3×10^{-4}

Note: Significant results are italicised in bold.

[a]Indicates the inter-annual thermocline deepening regime and was coded as 0 for manipulation years and 1 for reference years.

[b]Indicates the intra-annual thermocline deepening regime and was coded as 0 for reference years or pre-thermocline deepening during manipulation years, 1 for after the first thermocline deepening event within a manipulation year, 2 after the second thermocline deepening event, and 3 after the third thermocline deepening event.

[c]Assigned as a 0–1 indicator variable, where 0 was shallow peaks <3.6 m (median peak depth across 2016–2019) and 1 was deep peaks ≥3.6 m.

[d]Although an intense storm occurred on 5 May 2016, no ANOSIM test was conducted due to insufficient pre-storm data ($n = 1$ pre-storm sampling point).

In 2019, phytoplankton communities were substantially different between deep and shallow peaks (ANOSIM $R = 0.78$, $p = 6\times10^{-4}$; Figure 7f). Both 2017 and 2019 had more variability in peak depths than 2016 and 2018 (Figure S3i) and a greater abundance of cyanobacteria (primarily *Dolichospermum*) throughout the sampling season (Figure 5). In 2019, *Dolichospermum* was associated with shallow peaks and one diatom genus (*Asterionella*) was associated with deep peaks.

4 | DISCUSSION

Our 4-year whole-ecosystem manipulation revealed that an increased frequency of thermocline deepening events led to deeper phytoplankton biomass peaks at the inter-annual scale, and this effect was mediated by changes in thermal stratification and the depth of maximum SRP concentration in the photic zone. Responses of phytoplankton depth distributions to increased thermocline deepening frequency were consistent across summers, and desmids were consistently associated with reference summer conditions. However, other responses of phytoplankton to experimental thermocline deepening and extreme storm events, such as drivers of phytoplankton community composition, the magnitude of maximum biomass, and bloom occurrence, varied at both the inter-annual and intra-annual scale. Our results indicate that antecedent conditions (*sensu* Perga et al., 2018) and the seasonal timing of thermocline deepening may mediate the effect of abrupt thermocline deepening on phytoplankton community composition and distribution. Moreover, our finding that different taxa were associated with deep and shallow biomass peaks indicate that phytoplankton depth distributions and community composition are linked both across summers and within a summer. Below, we discuss our results in the context of predicting phytoplankton responses to the increased frequency of thermocline deepening anticipated under global change.

4.1 | How do phytoplankton depth distribution and community structure change in response to an increased frequency of thermocline deepening events?

Our findings indicate that an increased frequency of thermocline deepening events affected phytoplankton depth distributions via changes to physical and chemical gradients in the water column at the inter-annual scale. Thermocline deepening manipulations shifted distributions of Schmidt stability and buoyancy frequency towards less stratified conditions and led to increased variability in thermocline depth. Increased variability in thermocline depth probably results from entrainment of cooler hypolimnetic water, as a 3D hydrodynamic modelling study demonstrated that operation of the epilimnetic mixer in FCR in summer 2016 entrained water from just below the mixing system upward into the bubble

plume (Chen et al., 2018). Thermocline deepening manipulations also shifted the distribution of the depth of maximum SRP downward and led to increased variability of SRP depth distributions in the photic zone. In addition, the distribution of observed phytoplankton biomass peaks shifted deeper in manipulation summers, supporting the hypothesis shown in Figure 1b. These results were complemented by best-fit ARIMA models that consistently included thermal stratification metrics and the depth of maximum SRP as important predictors of the depth of phytoplankton biomass peaks. The finding that thermal stratification drives biomass peak depth aligns with previous research indicating that storms affect phytoplankton community structure via altered thermal stratification (Stockwell et al., 2020). Alteration of nutrient depth distributions in response to changes in thermocline depth also aligns with expectations from previous work on storms (e.g., Jennings et al., 2012), but, to our knowledge, the effects of these alterations in nutrient depth distributions on phytoplankton depth distributions at the whole-ecosystem scale has not been previously reported.

We found that more frequent thermocline deepening disrupted the ability of phytoplankton to respond to depth gradients of light. In reference years, light attenuation was the strongest predictor of peak depth and width, with higher light attenuation associated with both shallower and narrower biomass peaks. This result supports previous findings that light attenuation is the most important driver of deep chlorophyll maximum depth across a broad variety of lake types under stratified conditions (Leach et al., 2018). However, thermal stratification metrics (lake number for peak depth and buoyancy frequency for peak width) were the strongest predictors of peak depth and width in manipulation years, with stronger thermal stratification associated with shallower, narrower peaks in FCR. This finding is similar to results from a survey of phytoplankton depth distributions in 51 lakes in Québec, Canada (Lofton et al., 2020) and supports previous research regarding the importance of thermal stratification for formation of deep chlorophyll maxima (Cullen, 2015 and references therein). The importance of thermal stratification as a driver of phytoplankton depth distributions in years with weaker stratification indicates that a thermally stratified water column may be a prerequisite for phytoplankton depth distributions to respond to gradients in light.

Our study indicates that the depth distribution and community composition of phytoplankton are related, which may be linked to phytoplankton functional traits (*sensu* Litchman et al., 2007). Different phytoplankton taxa were associated with deep and shallow biomass peaks, and some of these associations may have been driven by trait-based responses to physicochemical conditions. For example, the filamentous cyanobacterium *Dolichospermum* was associated with shallow peaks across years, probably because that taxon is capable of both buoyancy regulation (Walsby, 1994) and nitrogen fixation (Wood et al., 2010), so it does not sink out of the water column and may persist in nitrogen-deficient surface waters. However, nitrogen fixation is metabolically expensive, often provides a relatively small percentage of nitrogen in phytoplankton standing stock, and usually does not eliminate nitrogen limitation of phytoplankton growth (Hayes et al., 2019); as a result, association of *Dolichospermum* with shallow biomass peaks may only occur once sufficient heterocysts have developed. By contrast, the cryptophyte *Cryptomonas* was associated with deeper peaks, possibly due to its low light tolerance (deNoyelles Jr et al., 2016) and ability to metabolise organic matter settling on the thermocline via mixotrophy (Mitra et al., 2016).

In other cases, the reasons for association of certain phytoplankton taxa with deep or shallow peaks were less clear. For example, *Rhodomonas* is functionally similar to *Cryptomonas* (Mitra et al., 2016), but was associated with shallow peaks in 2016–2019. The association of *Rhodomonas* with shallow peaks could be due to interspecific interactions of phytoplankton within the biomass peak. For example, mixotrophic *Rhodomonas* might metabolise organic carbon released via leaching or decomposition of *Dolichospermum* filaments accumulated in shallow peaks (Kritzberg et al., 2004; Ye et al., 2015). Recent research indicates that mixotrophy probably plays an important role in lake plankton dynamics (Beisner et al., 2019; Leles *et al* 2018), and may be important for determining community composition at the phytoplankton biomass peak in FCR.

4.2 | What are the duration and consistency of phytoplankton responses to thermocline deepening at intra-annual and inter-annual scales?

We found that phytoplankton community responses to experimental thermocline deepening and extreme storm events were variable both summer to summer and within a summer. Within years, we observed a dramatic shift in phytoplankton community structure following an extreme storm in 2019 and variable responses to individual manipulation events in 2016 and 2017. We also found a lack of correlation between observed exceptions to seasonal succession dynamics (e.g., changes in dominant taxa or the timing of maximum annual biomass relative to our expectations) and the number of thermocline deepening events per year. Altogether, these findings contradict expectations from previous research that the frequency of thermocline deepening events is of primary importance in determining phytoplankton community responses (Pannard et al., 2008; Reynolds et al., 1993) or shifting phytoplankton community structure in favour of mixing-tolerant taxa (Stockwell et al., 2020; Winder & Sommer, 2012).

Our results indicate that the antecedent conditions (e.g., strength of thermal stratification prior to a storm event) and seasonal timing of thermocline deepening events may be as important as their frequency in determining phytoplankton community responses. Across summers, different environmental drivers were associated with phytoplankton community composition at the depth of peak biomass in each year, maximum biomass was not different between manipulation and reference years, and the timing of blooms was

not associated with either thermocline deepening manipulations or storms. This lack of consistency in thermocline deepening responses across summers indicates that the effects of abrupt thermocline deepening on phytoplankton community composition may be mediated by other factors, such as winter ice cover, variability in seasonal catchment conditions, or inter- and intra-specific species interactions (Chase, 2003; Kritzberg et al., 2004; Perga et al., 2018; Stockwell et al., 2020; Thayne et al., 2021; Ye et al., 2015). Within each year, we found that disruption of established thermal stratification in summer (mid-June to mid-September) caused greater disruption to phytoplankton communities than in late spring (May to early June) when stratification is weaker. This finding supports the framework proposed by Stockwell et al. (2020), which predicts that the response of phytoplankton to storm events is mediated by their functional traits (e.g., buoyancy, growth rate, mixotrophy). While spring and early autumn plankton communities in temperate lakes might be well-adapted to mixing and changes in stratification, summer communities are probably not (de Senerpont Domis et al., 2013), and so a mid-summer thermocline deepening event could lead to greater change in community structure. Alternatively, differences in phytoplankton community structure after an intense storm in 2019 may be due to storm effects that we could not reproduce via thermocline deepening manipulations.

The relative consistency in seasonal succession among all years indicates that intermittent, abrupt thermocline deepening does not completely disrupt seasonal succession. This consistency is supported by the lack of significant differences in June and September communities among years. Moreover, the occurrence of *Dolichospermum* and *Cryptomonas*, the two most dominant taxa during our study period, in July and August phytoplankton communities across years further indicates that functional associations of phytoplankton taxa (*sensu* Reynolds et al., 2002) tend to occur consistently at particular times of year, regardless of the frequency of thermocline deepening. For example, we observed a succession of phytoplankton taxa at the peak depth typical of small, mesotrophic–eutrophic temperate lakes (following de Senerpont Domis et al., 2013; Reynolds et al., 2002; Sommer et al., 1986), where late spring communities of diatoms and chrysophytes (e.g., *Asterionella*, *Dinobryon*) are succeeded by small-celled chlorophytes and cyanobacteria in early summer, followed by dominance (and sometimes blooms) of nitrogen-fixing cyanobacteria starting in July (e.g., *Dolichospermum*). These assemblages dominated by filamentous cyanobacteria usually represent the annual biomass maximum, and finally shift to assemblages characterised by mixotrophic taxa (e.g., *Cryptomonas*, *Prorocentrum*) in August and September.

Increases in thermocline deepening frequency did not appear to be the primary driver of deviations from seasonal succession, as notable exceptions to successional dynamics occurred both in 2016 (four deepening events; the annual biomass maximum occurred in August and comprised primarily *Cryptomonas*) and in 2019 (one deepening event; *Dolichospermum* dominated the phytoplankton community continuously following the extreme storm on 8 June 2019). The robustness of seasonal succession dynamics despite our experimental manipulations and extreme storm events indicates the potential importance of multiple mechanisms, including littoral propagule seed banks, overland dispersal, and top-down control by zooplankton grazing, in maintaining phytoplankton seasonal succession (Cottingham et al., 2021; Padisák et al., 2016; Sommer et al., 2012).

4.3 | Limitations and future opportunities

While our study provides insight into the inter-annual and intra-annual responses of phytoplankton communities to intermittent, abrupt thermocline deepening, some limitations must be considered. There were several differences between the effects of our experimental thermocline deepening manipulations and extreme storm effects on lake ecosystems. First, we were unable to reproduce storm effects such as increased inflow and nutrient loading or changes in epilimnetic water temperature (e.g., Doubek et al., 2021; Klug et al., 2012; Stockwell et al., 2020). Second, FCR's engineered mixing system is installed at a depth of 5 m, or at approximately the middle of the water column, so mixing action is initiated from the middle of the water column rather than the surface, as would occur due to a storm. However, examination of two naturally occurring extreme storm events confirmed that our thermocline deepening manipulations were a reasonable representation of thermocline deepening due to natural storms, and that both storm-driven mixing and epilimnetic mixing manipulations caused turnover in phytoplankton community composition at the depth of peak biomass at the intra-annual scale.

There are also limitations conferred by our sampling programme and experimental design. First, phytoplankton depth distributions were probably influenced by factors in addition to thermocline deepening, including inter-annual differences in water residence time, precipitation, and other factors contributing to natural year-to-year variability in phytoplankton communities, which can be especially pronounced in reservoirs (Hayes et al., 2017). Second, our weekly field sampling protocol precluded analysis of patterns of phytoplankton community dynamics at sub-weekly timescales, which may be particularly important for understanding short-term phytoplankton response to storms (Stockwell et al., 2020). In particular, the importance of microscale turbulence (Li et al., 2018; Wu et al., 2019) and convective processes (Bouffard & Wüest, 2019) in movement of phytoplankton cells and formation of surface blooms at short timescales is well-documented, although not quantified in this study. However, the fact that we still observed consistent differences in phytoplankton depth distributions between manipulation and reference years supports the strength of our results and approach. Third, an alternative experimental design, such as alternating summers with and without experimental manipulations, might have permitted more robust comparison of manipulation and reference summers. However, our experimental design was limited by drinking water quality management requirements, and still enabled assessment of increased thermocline deepening frequency over multiple sequential summers.

Our findings indicate that examination of the effects of antecedent conditions and seasonal timing of storms on phytoplankton responses and consideration of inter-specific interactions in biomass peaks

provide promising avenues for future research. Explicit consideration of how precipitation, water residence time, phytoplankton propagule seed banks, pre-storm thermal stratification strength, and other antecedent conditions affect phytoplankton community response to abrupt thermocline deepening could enhance our understanding of future phytoplankton response to increased frequency and intensity of storms (e.g., Cottingham et al., 2021; Thayne et al., 2021). In addition, our finding that some phytoplankton taxa are associated with peak depths that do not align with theoretical expectations based on functional traits indicates that further attention may be needed on the role of inter-specific interactions of phytoplankton taxa (e.g., Posch et al., 2015) in the formation of phytoplankton depth distributions.

4.4 | CONCLUSIONS

Our work demonstrates that an increased frequency of thermocline deepening events may alter both phytoplankton depth distributions (following Figure 1b) and community structure via alteration of physical and chemical environmental conditions at the inter-annual scale. Furthermore, our findings support previous research indicating that phytoplankton depth distribution and community composition are linked at both the inter-annual and intra-annual scale. Finally, we show that responses of phytoplankton community composition to intermittent, abrupt thermocline deepening are not consistent summer to summer or among thermocline deepening events within a summer, indicating that antecedent conditions probably play an important role in mediating phytoplankton responses to increased frequency and intensity of storms under global change. Overall, our findings emphasise that the spatial distribution and composition of freshwater phytoplankton communities are sensitive to thermocline deepening both across and within summers, and so both distribution and composition must be considered when predicting phytoplankton responses to storms under global change.

AUTHOR CONTRIBUTIONS

Conceptualisation and developing methods: M.E.L., R.P.M., and C.C.C. designed the whole-ecosystem manipulation field campaign. Conducting the research: all authors helped with collection and collation of field data. Analytical chemistry was conducted by M.E.L., D.W.H., H.L.W., and W.M.W; CTD data collection was led by R.P.M. and A.S.L; and all authors assisted with publication of field datasets. The field sampling programme was coordinated by M.E.L., R.P.M., A.G.H., and C.C.C. Data analysis: M.E.L. conducted all statistical analyses. Data interpretation, preparation of figures and tables, writing: M.E.L. drafted the manuscript with C.C.C., D.W.H., and R.P.M. All authors read and approved the final version of the manuscript.

ACKNOWLEDGMENTS

We thank the Western Virginia Water Authority for access to field sites, Barbara Niederlehner for assistance with analytical chemistry, and Kylie Campbell, Leah Finegold, Niall Goard, Miles Goodall, Charlotte Harrell, James Maze, Ashley Mickens, Beatrice Scott, Jacob Wynne, Claire Vavrus, Shengyang Chen, Jon Doubek, Kait Farrell, Katie Krueger, and Nicole Ward for help with field work. We also thank Bryan Brown, Erin Hotchkiss, Madeline Schreiber, and members of the Virginia Tech Reservoir Group and Global Change Center for helpful feedback, as well as Beatrix Beisner and Taylor Leach for valuable discussions on phytoplankton vertical distributions.

FUNDING INFORMATION

Funding was provided by NSF grants CNS-1737424, DEB-1753639, DBI-1933016, DBI-1933102, and DGE-1651272, the Western Virginia Water Authority, the Global Change Center at Virginia Tech, the Virginia Tech College of Science Roundtable Make-A-Difference Scholarship, and the Virginia Water Resources Research Center.

CONFLICT OF INTEREST

The authors declare no conflicts of interest.

DATA AVAILABILITY STATEMENT

All data associated with this study are published in the Environmental Data Initiative repository and are cited in the text (Carey, 2021; Carey et al., 2020 2020b, 2021b, 2021c 2021d 2021e; Lofton et al., 2021). All analysis code is available on GitHub (https://github.com/melofton/FCR-phytos) and published via Zenodo (DOI: 10.5281/zenodo.6483433).

ORCID

Mary E. Lofton https://orcid.org/0000-0003-3270-1330
Dexter W. Howard https://orcid.org/0000-0002-6118-2149

REFERENCES

Acker, F. (2002). Protocol P-13-52 Analysis of USGS NAWQA Program Phytoplankton Samples. In D. F. Charles, C. Knowles, & R. S. Davis (Eds.), *Protocols for the analysis of algal samples collected as part of the U.S. Geological Survey National Water-Quality Assessment Program* (pp. 87–96). The Academy of Natural Sciences: Patrick Center for Environmental Research–Phycology Section.

Beisner, B. E., Grossart, H. P., & Gasol, J. M. (2019). A guide to methods for estimating phago-mixotrophy in nanophytoplankton. *Journal of Plankton Research*, *41*, 77–89. https://doi.org/10.1093/plankt/fbz008

Beisner, B. E., & Longhi, M. L. (2013). Spatial overlap in lake phytoplankton: Relations with environmental factors and consequences for diversity. *Limnology and Oceanography*, *58*, 1419–1430. https://doi.org/10.4319/lo.2013.58.4.1419

Beutler, M., Wiltshire, K. H., Meyer, B., Moldaenke, C., Lüring, C., Meyerhöfer, M., … Dau, H. (2002). A fluorometric method for the differentiation of algal populations in vivo and in situ. *Photosynthesis Research*, *72*, 39–53. https://doi.org/10.1023/A:1016026607048

Bouffard, D., & Wüest, A. (2019). Convection in lakes. *Annual Review of Fluid Mechanics*, *51*, 189–215. https://doi.org/10.1146/annurev-fluid-010518-040506

Brierley, B., Carvalho, L., Davies, S., & Krokowski, J. (2007). *Guidance on the quantitative analysis of phytoplankton in freshwater samples*. European Water Framework Directive.

Burnham, K. P., & Anderson, D. R. (2002). *Model selection and multimodel inference: A practical information-theoretic approach* (2nd ed.). Springer.

Cantin, A., Beisner, B. E., Gunn, J. M., Prairie, Y. T., & Winter, J. G. (2011). Effects of thermocline deepening on lake plankton communities. *Canadian Journal of Fisheries and Aquatic Sciences*, *68*, 260–276. https://doi.org/10.1139/F10-138

Carey C.C. (2021). *Ice cover data for Falling Creek Reservoir, Vinton, Virginia, USA for 2013-2021 ver. 3*. Environmental Data Initiative. https://doi.org/10.6073/pasta/a23233527aa90638b2cd3075627c91e6

Carey C.C., Breef-Pilz A., Bookout B.J., Lofton M.E. & McClure R.P. (2021). *Time series of high-frequency meteorological data at Falling Creek Reservoir, Virginia, USA 2015-2020 ver. 5*. Environmental Data Initiative. https://doi.org/10.6073/pasta/890e4c11f4348b3ceda802732ffa48b4

Carey, C.C., A.B. Gerling, J.P. Doubek, K.D. Hamre, R.P. McClure, M.E. Lofton, & K.J. Farrell (2020). *Secchi depth data and discrete depth profiles of photosynthetically active radiation, temperature, dissolved oxygen, and pH for Beaverdam Reservoir, Carvins Cove Reservoir, Falling Creek Reservoir, Gatewood Reservoir, and Spring Hollow Reservoir in southw*. Environmental Data Initiative. https://doi.org/10.6073/pasta/3e9f27971e353c8a80840b5e99a67d0c

Carey, C. C., Ibelings, B. W., Hoffmann, E. P., Hamilton, D. P., & Brookes, J. D. (2012). Eco-physiological adaptations that favour freshwater cyanobacteria in a changing climate. *Water Research*, *46*, 1394–1407. https://doi.org/10.1016/j.watres.2011.12.016

Carey, C. C., Lewis, A. S., McClure, R. P., Gerling, A. B., Chen, S., Das, A., … Wander, H. L. (2021). *Time series of high-frequency profiles of depth, temperature, dissolved oxygen, conductivity, specific conductivity, chlorophyll a, turbidity, pH, oxidation-reduction potential, photosynthetic active radiation, and descent rate for Beaverdam Reservoir, Ca*. Environmental Data Initiative. https://doi.org/10.6073/pasta/5448f9d415fd09e0090a46b9d4020ccc

Carey C.C., Lofton M.E., Woelmer W.M., Hamre K.D., Doubek J.P. & McClure R.P. (2021). *Time-series of high-frequency profiles of fluorescence-based phytoplankton spectral groups in Beaverdam Reservoir, Carvins Cove Reservoir, Falling Creek Reservoir, Gatewood Reservoir, and Spring Hollow Reservoir in southwestern Virginia, USA 2014-2020 ver*. Environmental Data Initiative. https://doi.org/10.6073/pasta/54d4bd2fee1e52e36e2b0f230912d2da

Carey, C.C., H.L. Wander, W.M. Woelmer, M.E. Lofton, A.B. Gerling, R.P. McClure, … K.J. Farrell (2020). *Water chemistry time series for Beaverdam Reservoir, Carvins Cove Reservoir, Falling Creek Reservoir, Gatewood Reservoir, and Spring Hollow Reservoir in southwestern Virginia, USA 2013-2019 ver 7*. Environmental Data Initiative. https://doi.org/10.6073/pasta/0d29704769868facec3e238e64d35557

Carey C.C., Woelmer W.M.., Lewis A.S.L., Breef-Pilz A., Howard D.W. & Bookout B.J. (2021). *Time series of high-frequency sensor data measuring water temperature, dissolved oxygen, pressure, conductivity, specific conductance, total dissolved solids, chlorophyll a, phycocyanin, and fluorescent dissolved organic matter at discrete depths in Falling Creek Reservoir, Virginia, USA in 2018-2020*. Environmental Data Initiative. https://doi.org/10.6073/pasta/88896f4a7208c9b7bddcf498258edf78

Carlson, R., & Simpson, J. (1996). *A coordinator's guide to volunteer lake monitoring methods*. North American Lake Management Society.

Catherine, A., Escoffier, N., Belhocine, A., Nasri, A. B., Hamlaoui, S., Yéprémian, C., … Troussellier, M. (2012). On the use of the FluoroProbe®, a phytoplankton quantification method based on fluorescence excitation spectra for large-scale surveys of lakes and reservoirs. *Water Research*, *46*, 1771–1784.

Chase, J. M. (2003). Community assembly: When should history matter? *Oecologia*, *136*, 489–498. https://doi.org/10.1007/s00442-003-1311-7

Chen, S., Little, J. C., Carey, C. C., McClure, R. P., Lofton, M. E., & Lei, C. (2018). Three-dimensional effects of artificial mixing in a shallow drinking-water reservoir. *Water Resources Research*, *54*, 425–441. https://doi.org/10.1002/2017WR021127

Chorus, I., & Welker, M. (Eds.). (2021). *Toxic cyanobacteria in water: A guide to their public health consequences, monitoring and management*. Taylor & Francis.

Connell, J. H. (1978). Diversity in tropical rain forests and coral reefs: High diversity of trees and corals is maintained only in a nonequilibrium state. *Science*, *199*, 1302–1310. https://doi.org/10.2307/1745369

Cottingham, K. L., Ewing, H. A., Greer, M. L., Carey, C. C., & Weathers, K. C. (2015). Cyanobacteria as biological drivers of lake nitrogen and phosphorus cycling. *Ecosphere*, *6*, 1–19. https://doi.org/10.1890/ES14-00174.1

Cottingham, K. L., Weathers, K. C., Ewing, H. A., Greer, M. L., & Carey, C. C. (2021). Predicting the effects of climate change on freshwater cyanobacterial blooms requires consideration of the complete cyanobacterial life cycle. *Journal of Plankton Research*, *43*, 10–19. https://doi.org/10.1093/plankt/fbaa059

Crumpton, W. G. (1987). A simple and reliable method for making permanent mounts of phytoplankton for light and fluorescence microscopy. *Limnology and Oceanography*, *32*, 1154–1159. https://doi.org/10.4319/lo.1987.32.5.1154

Cullen, J. J. (2015). Subsurface chlorophyll maximum layers: Enduring enigma or mystery solved? *Annual Review of Marine Science*, *7*, 207–239. https://doi.org/10.1146/annurev-marine-010213-135111

Danielsdottir, M. G., Brett, M. T., & Arhonditsis, G. B. (2007). Phytoplankton food quality control of planktonic food web processes. *Hydrobiologia*, *589*, 29–41. https://doi.org/10.1007/s10750-007-0714-6

De Cáceres M., Jansen F. & Dell N. (2020). *Package 'indicspecies' v 1.7.9: Relationship between species and groups of sites*. Comprehensive R Archive Network (CRAN). https://doi.org/10.1890/08-1823.1

De Cáceres, M., Legendre, P., & Moretti, M. (2010). Improving indicator species analysis by combining groups of sites. *Oikos*, *119*, 1674–1684. https://doi.org/10.1111/j.1600-0706.2010.18334.x

De Senerpont Domis, L. N., Elser, J. J., Gsell, A. S., Huszar, V. L., Ibelings, B. W., Jeppesen, E., … Van Donk, E. (2013). Plankton dynamics under different climatic conditions in space and time. *Freshwater Biology*, *58*, 463–482. https://doi.org/10.1111/fwb.12053

deNoyelles, F., Jr., Smith, V. H., Kastens, J. H., Bennett, L., Lomas, J. M., Knapp, C. W., … Graham, D. W. (2016). A 21-year record of vertically migrating subepilimnetic populations of *Cryptomonas* spp. *Inland Waters*, *6*, 172–184. https://doi.org/10.5268/IW-6.2.930

Diaz, R. J. (2001). Overview of hypoxia around the world. *Journal of Environmental Quality*, *30*, 275–281. https://doi.org/10.2134/jeq2001.302275x

Diehl, S., Berger, S., Ptacnik, R., & Wild, A. (2002). Phytoplankton, light, and nutrients in a gradient of mixing depths: Field experiments. *Ecology*, *83*, 399–411.

Dokulil, M. T., de Eyto, E., Maberly, S. C., May, L., Weyhenmeyer, G. A., & Woolway, R. I. (2021). Increasing maximum lake surface temperature under climate change. *Climatic Change*, *165*, 1–17. https://doi.org/10.1007/s10584-021-03085-1

Donohue, I., & Garcia, M. J. (2009). Impacts of increased sediment loads on the ecology of lakes. *Biological Reviews*, *84*, 517–531. https://doi.org/10.1111/j.1469-185X.2009.00081.x

Doubek, J. P., Anneville, O., Dur, G., Lewandowska, A. M., Patil, V. P., Rusak, J. A., … Venail, P. (2021). The extent and variability of storm-induced temperature changes in lakes measured with long-term and high-frequency data. *Limnology and Oceanography*, *9999*, 1–14. https://doi.org/10.1002/lno.11739

Flaim, G., Eccel, E., Zeileis, A., Toller, G., Cerasino, L., & Obertegger, U. (2016). Effects of re-oligotrophication and climate change on lake thermal structure. *Freshwater Biology*, *61*, 1802–1814. https://doi.org/10.1111/fwb.12819

Fox, J. W. (2013). The intermediate disturbance hypothesis should be abandoned. *Trends in Ecology and Evolution*, *28*, 86–92. https://doi.org/10.1016/j.tree.2012.08.014

Garneau, M.-E., Posch, T., Hitz, G., Siegwart, R., & Pernthaler, J. (2013). Short-term displacement of Planktothrix rubescens (cyanobacteria) in a pre-alpine lake observed using an autonomous sampling platform, *58*, 1892–1906. https://doi.org/10.4319/lo.2013.58.5.1892

Gray, E., Elliott, J. A., Mackay, E. B., Folkard, A. M., Keenan, P. O., & Jones, I. D. (2019). Modelling lake cyanobacterial blooms: Disentangling the climate-driven impacts of changing mixed depth and water temperature. *Freshwater Biology*, *64*, 2141–2155. https://doi.org/10.1111/fwb.13402

Hamilton, D. P., Brien, K. R. O., & McBride, C. G. (2010). Vertical distributions of chlorophyll in deep, warm monomictic lakes. *Aquatic Sciences*, *72*, 295–307. https://doi.org/10.1007/s00027-010-0131-1

Hayes, N. M., Deemer, B. R., Corman, J. R., Razavi, N. R., & Strock, K. E. (2017). Key differences between lakes and reservoirs modify climate signals: A case for a new conceptual model. *Limnology and Oceanography Letters*, *2*, 47–62. https://doi.org/10.1002/lol2.10036

Hayes, N. M., Patoine, A., Haig, H. A., Simpson, G. L., Swarbrick, V. J., Wiik, E., & Leavitt, P. R. (2019). Spatial and temporal variation in nitrogen fixation and its importance to phytoplankton in phosphorus-rich lakes. *Freshwater Biology*, *64*, 269–283. https://doi.org/10.1111/fwb.13214

Henson, S. A., Cole, H. S., Hopkins, J., Martin, A. P., & Yool, A. (2018). Detection of climate change-driven trends in phytoplankton phenology. *Global Change Biology*, *24*, e101–e111. https://doi.org/10.1111/gcb.13886

Hillebrand, H., Dürselen, C.-D., Kirschtel, D., Pollingher, U., & Zohary, T. (1999). Biovolume calculation for pelagic and benthic microalgae. *Journal of Phycology*, *35*, 403–424. https://doi.org/10.1046/j.1529-8817.1999.3520403.x

Ho, J. C., & Michalak, A. M. (2020). Exploring temperature and precipitation impacts on harmful algal blooms across continental U.S. lakes. *Limnology and Oceanography*, *65*, 992–1009. https://doi.org/10.1002/lno.11365

Ho, J. C., Michalak, A. M., & Pahlevan, N. (2019). Widespread global increase in intense lake phytoplankton blooms since the 1980s. *Nature*, *574*, 667–670. https://doi.org/10.1038/s41586-019-1648-7

Holm, S. (1979). A simple sequentially rejective multiple test procedure. *Scandinavian Journal of Statistics*, *6*, 65–70.

Huisman, J., Sharples, J., Stroom, J. M., Visser, P. M., Kardinaal, W. E., Verspagen, J. M., & Sommeijer, B. (2004). Changes in turbulent mixing shift competition for light between phytoplankton species. *Ecology*, *85*, 2960–2970.

Hyndman R., Athanasopoulos G., Bergmeir C., Caceres G., Chhay L., O'Hara-Wild, M … Zhou, Z. (2021). *forecast: Forecasting functions for time series and linear models*. Comprehensive R Archive Network (CRAN).

Hyndman, R., & Khandakar, Y. (2008). Automatic time series forecasting: The forecast package for R. *Journal of Statistical Software*, *26*, 1–22.

Hyndman, R. J., & Athanasopoulos, G. (2018). *Forecasting: Principles and practice* (2nd ed.). Otexts.

Jennings, E., Jones, S., Arvola, L., Staehr, P. A., Gaiser, E., Jones, I. D., … De Eyto, E. (2012). Effects of weather-related episodic events in lakes: An analysis based on high-frequency data. *Freshwater Biology*, *57*, 589–601. https://doi.org/10.1111/j.1365-2427.2011.02729.x

Jobin, V. O., & Beisner, B. E. (2014). Deep chlorophyll maxima, spatial overlap and diversity in phytoplankton exposed to experimentally altered thermal stratification. *Journal of Plankton Research*, *36*, 933–942. https://doi.org/10.1093/plankt/fbu036

Kasprzak, P., Shatwell, T., Gessner, M. O., Gonsiorczyk, T., Kirillin, G., Selmeczy, G., … Engelhardt, C. (2017). Extreme weather event triggers cascade towards extreme turbidity in a clear-water lake. *Ecosystems*, *20*, 1–14. https://doi.org/10.1007/s10021-017-0121-4

Kirchmeier-Young, M. C., & Zhang, X. (2020). Human influence has intensified extreme precipitation in North America. *Proceedings of the National Academy of Sciences of the United States of America*, *117*, 13308–13313. https://doi.org/10.1073/pnas.1921628117

Klausmeier, C. A., & Litchman, E. (2001). Algal games: The vertical distribution of phytoplankton in poorly mixed water columns. *Limnology and Oceanography*, *46*, 1998–2007.

Klug, J. L., Richardson, D. C., Ewing, H. A., Hargreaves, B. R., Samal, N. R., Vachon, D., … Weathers, K. C. (2012). Ecosystem effects of a tropical cyclone on a network of lakes in northeastern North America. *Environmental Science & Technology*, *46*, 11693–11701. https://doi.org/10.1021/es302063v

Kraemer, B. M., Anneville, O., Chandra, S., Dix, M., Kuusisto, E., Livingstone, D. M., … Tamatamah, R. (2015). Morphometry and average temperature affect lake stratification responses to climate change. *Geophysical Research Letters*, *42*, 4981–4988. https://doi.org/10.1002/2015GL064097

Kritzberg, E. S., Cole, J. J., Pace, M. L., Granéli, W., & Bade, D. L. (2004). Autochthonous versus allochthonous carbon sources of bacteria: Results from whole-lake 13C addition experiments. *Limnology and Oceanography*, *49*, 588–596. https://doi.org/10.4319/lo.2004.49.2.0588

Latasa, M., Cabello, A. M., Morán, X. A. G., Massana, R., & Scharek, R. (2017). Distribution of phytoplankton groups within the deep chlorophyll maximum. *Limnology and Oceanography*, *62*, 665–685. https://doi.org/10.1002/lno.10452

Leach, T. H., Beisner, B. E., Carey, C. C., Pernica, P., Rose, K. C., Huot, Y., … Jacquet, S. (2018). Patterns and drivers of deep chlorophyll maxima structure in 100 lakes: The relative importance of light and thermal stratification. *Limnology and Oceanography*, *63*, 628–646. https://doi.org/10.1002/lno.10656

Leles, S. G., Polimene, L., Bruggeman, J., Blackford, J., Ciavatta, S., Mitra, A., & Flynn, K. J. (2018). Modelling mixotrophic functional diversity and implications for ecosystem function. *Journal of Plankton Research*, *40*, 627–642. https://doi.org/10.1093/plankt/fby044

Li, M., Xiao, M., Zhang, P., & Hamilton, D. P. (2018). Morphospecies-dependent disaggregation of colonies of the cyanobacterium *Microcystis* under high turbulent mixing. *Water Research*, *141*, 340–348. https://doi.org/10.1016/j.watres.2018.05.017

Litchman, E., Klausmeier, C. A., Schofield, O. M., & Falkowski, P. G. (2007). The role of functional traits and trade-offs in structuring phytoplankton communities: Scaling from cellular to ecosystem level. *Ecology Letters*, *10*, 1170–1181. https://doi.org/10.1111/j.1461-0248.2007.01117.x

Lofton, M.E., D.W. Howard, R.P. McClure, H.L. Wander, W.M. Woelmer, A.G. Hounshell, … C.C. Carey (2021). *Time series of phytoplankton biovolume at the depth of the vertical chlorophyll maximum in Falling Creek Reservoir, Vinton, VA, USA 2016-2019*. Environmental Data Initiative. https://doi.org/10.6073/pasta/2de760e8b72e474c31e42526f5360f9a

Lofton, M. E., Leach, T. H., Beisner, B. E., & Carey, C. C. (2020). Relative importance of top-down vs. bottom-up control of lake phytoplankton vertical distributions varies among fluorescence-based spectral groups. *Limnology and Oceanography*, *9999*, 1–17. https://doi.org/10.1002/lno.11465

Lofton, M. E., McClure, R. P., Chen, S., Little, J. C., & Carey, C. C. (2019). Whole-ecosystem experiments reveal varying responses of phytoplankton functional groups to epilimnetic mixing in a eutrophic reservoir. *Water*, *11*, 222. https://doi.org/10.3390/w11020222

Longhi, M. L., & Beisner, B. E. (2009). Environmental factors controlling the vertical distribution of phytoplankton in lakes. *Journal of Plankton Research*, *31*, 1195–1207.

Lydersen, E., & Andersen, T. (2007). Ecosystem effects of thermal manipulation of a whole lake, Lake Breisjøen, southern Norway (THERMOS project). *Hydrology and Earth System Sciences*, *12*, 509–522. https://doi.org/10.5194/hessd-4-3357-2007

McCune B. & Grace J.B. (2002). *Analysis of ecological communities*. MjM Software Design, Gleneden Beach, OR SE - iv, 300 pages: Illustrations; 28 cm.

Mitra, A., Flynn, K. J., Tillmann, U., Raven, J. A., Caron, D., Stoecker, D. K., … Wilken, S. (2016). Defining planktonic protist functional groups on mechanisms for energy and nutrient acquisition: Incorporation of diverse mixotrophic strategies. *Annals of Anatomy*, *167*, 106–120. https://doi.org/10.1016/j.protis.2016.01.003

Oksanen J, Blanchet FG, Kindt R, Legendre P, Minchin PR, O'Hara RB, … Oksanen MJ (2020). *Package 'vegan' v. 2.5-7: Community ecology package*. Comprehensive R Archive Network (CRAN).

O'Reilly, C. M., Sharma, S., Gray, D. K., Hampton, S. E., Read, J. S., Rowley, R. J., … Weyhenmeyer, G. A. (2015). Rapid and highly variable warming of lake surface waters around the globe. *Geophysical Research Letters*, *42*, 773–781. https://doi.org/10.1002/2015GL066235.Received

Padisák, J., Vasas, G., & Borics, G. (2016). Phycogeography of freshwater phytoplankton: Traditional knowledge and new molecular tools. *Hydrobiologia*, *764*, 3–27. https://doi.org/10.1007/s10750-015-2259-4

Pannard, A., Bormans, M., & Lagadeuc, Y. (2008). Phytoplankton species turnover controlled by physical forcing at different time scales. *Canadian Journal of Fisheries and Aquatic Sciences*, *65*, 47–60. https://doi.org/10.1139/F07-149

Perga, M. E., Bouffard, D., Bruel, R., Rodriguez, L., & Guénand, Y. (2018). Storm impacts on alpine lakes: Antecedent weather conditions matter more than the event intensity. *Global Change Biology*, *24*, 5004–5016. https://doi.org/10.1111/gcb.14384

Planas, D., & Paquet, S. (2016). Importance of climate change-physical forcing on the increase of cyanobacterial blooms in a small, stratified lake. *Journal of Limnology*, *75*, 201–214. https://doi.org/10.4081/jlimnol.2016.1371

Posch, T., Eugster, B., Pomati, F., Pernthaler, J., Pitsch, G., & Eckert, E. M. (2015). Network of interactions between ciliates and phytoplankton during spring. *Frontiers in Microbiology*, *6*, 1–14. https://doi.org/10.3389/fmicb.2015.01289

Razali, N. M., & Wah, Y. B. (2011). Power comparisons of Shapiro-Wilk, Kolmogorov-Smirnov, Lilliefors and Anderson-Darling tests, *2*, 21–33.

Reinl, K. L., Sterner, R. W., & Austin, J. A. (2020). Seasonality and physical drivers of deepth chlorophyll layers in Lake Superior, with implications for a rapidly warming lake. *Journal of Great Lakes Research*, *46*, 1615–1624.

Ren, M., Eyto, E., De, D. M., Poole, R., & Jennings, E. (2020). 13 years of storms: An analysis of the effects of storms on lake physics on the Atlantic Fringe of Europe. *Water*, *12*, 318. https://doi.org/10.3390/w12020318

Reynolds, C. S., Huszar, V., Kruk, C., Naselli-Flores, L., & Melo, S. (2002). Towards a functional classification of the freshwater phytoplankton. *Journal of Plankton Research*, *24*, 417–428. https://doi.org/10.1093/plankt/24.5.417

Reynolds, C. S., Padisák, J., & Sommer, U. (1993). Intermediate disturbance in the ecology of phytoplankton and the maintenance of species diversity: A synthesis. *Hydrobiologia*, *249*, 183–188.

Rinke, K., Huber, A. M., Kempke, S., Eder, M., Wolf, T., Probst, W. N., … Rothhaupta, K. O. (2009). Lake-wide distributions of temperature, phytoplankton, zooplankton, and fish in the pelagic zone of a large lake. *Limnology and Oceanography*, *54*, 1306–1322.

Smith, V. H. (2003). Eutrophication of freshwater and coastal marine ecosystems a global problem. *Environmental Science and Pollution Research*, *10*, 126–139. https://doi.org/10.1065/espr2002.12.142

Sommer, U., Adrian, R., De Senerpont Domis, L., Elser, J. J., Gaedke, U., Ibelings, B., … Van Donk, E. (2012). Beyond the Plankton Ecology Group (PEG) model: Mechanisms driving plankton succession. *Annual Review of Ecology, Evolution, and Systematics*, *43*, 429–448. https://doi.org/10.1146/annurev-ecolsys-110411-160251

Sommer, U., Gliwicz, Z. M., Lampert, W., & Duncan, A. (1986). The PEG*-model of seasonal succession of planktonic events in fresh water. *Archiv für Hydrobiologie*, *106*, 433–471.

Stockwell, J. D., Doubek, J. P., Adrian, R., Anneville, O., Carey, C. C., Carvalho, L., … Ibelings, B. W. (2020). Storm impacts on phytoplankton community dynamics in lakes. *Global Change Biology*, *26*, 2756–2784. https://doi.org/10.1111/gcb.15033

Thayne, M. W., Kraemer, B. M., Mesman, J. P., Ibelings, B. W., & Adrian, R. (2021). Antecedent lake conditions shape resistance and resilience of a shallow lake ecosystem following extreme wind storms. *Limnology and Oceanography*, *9999*, 1–20. https://doi.org/10.1002/lno.11859

Visser, P. M., Ibelings, B. W., Bormans, M., & Huisman, J. (2016). Artificial mixing to control cyanobacterial blooms: A review. *Aquatic Ecology*, *50*, 423–441. https://doi.org/10.1007/s10452-015-9537-0

Walsby, A. E. (1994). Gas vesicles. *Microbiological Reviews*, *58*, 94–144. https://doi.org/10.1146/annurev.pp.26.060175.002235

Watson, S., Monis, P., Baker, P., & Giglio, S. (2016). Biochemistry and genetics of taste- and odor-producing cyanobacteria. *Harmful Algae*, *54*, 112–127. https://doi.org/10.1016/j.hal.2015.11.008

Wetzel, R. G., & Likens, G. E. (1991). *Limnological analyses* (2nd ed.). Springer-Verlag.

Winder, M., & Sommer, U. (2012). Phytoplankton response to a changing climate. *Hydrobiologia*, *698*, 5–16. https://doi.org/10.1007/s10750-012-1149-2

Winslow L, Read J, Woolway R, Brentrup J, Leach T, Zwart J, … Collinge D (2019). *rLakeAnalyzer: Lake physics tools*. Comprehensive R Archive Network (CRAN).

Wood, S. A., Prentice, M. J., Smith, K., & Hamilton, D. P. (2010). Low dissolved inorganic nitrogen and increased heterocyte frequency: Precursors to Anabaena planktonica blooms in a temperate, eutrophic reservoir. *Journal of Plankton Research*, *32*, 1315–1325. https://doi.org/10.1093/plankt/fbq048

Woolway, R. I., & Merchant, C. J. (2019). Worldwide alteration of lake mixing regimes in response to climate change. *Nature Geoscience*, *12*, 271–276. https://doi.org/10.1038/s41561-019-0322-x

Wu, T., Qin, B., Brookes, J. D., Shi, K., Zhu, G., Zhu, M., … Wang, Z. (2015). The influence of changes in wind patterns on the areal extension of surface cyanobacterial blooms in a large shallow lake in China. *Science of the Total Environment*, *518–519*, 24–30.

Wu, X., Noss, C., Liu, L., & Lorke, A. (2019). Effects of small-scale turbulence at the air-water interface on microcystis surface scum formation. *Water Research*, *167*, 115091. https://doi.org/10.1016/j.watres.2019.115091

Ye, L., Wu, X., Liu, B., Yan, D., & Kong, F. (2015). Dynamics and sources of dissolved organic carbon during phytoplankton bloom in hyper-eutrophic Lake Taihu (China). *Limnologica*, *54*, 5–13. https://doi.org/10.1016/j.limno.2015.05.003

SUPPORTING INFORMATION

Additional supporting information can be found online in the Supporting Information section at the end of this article.

How to cite this article: Lofton, M. E., Howard, D. W., McClure, R. P., Wander, H. L., Woelmer, W. M., Hounshell, A. G., Lewis, A. S. L., & Carey, C. C. (2022). Experimental thermocline deepening alters vertical distribution and community structure of phytoplankton in a 4-year whole-reservoir manipulation. *Freshwater Biology*, *67*, 1903–1924. https://doi.org/10.1111/fwb.13983